



HAL
open science

Chemical weathering of mafic rocks in boreal subarctic environment (northwest Russia) under influence of glacial moraine deposits

Ekaterina V. Vasyukova, Priscia Oliva, Jerome Viers, Francois Martin, Bernard Dupré, Oleg S. Pokrovsky

► To cite this version:

Ekaterina V. Vasyukova, Priscia Oliva, Jerome Viers, Francois Martin, Bernard Dupré, et al.. Chemical weathering of mafic rocks in boreal subarctic environment (northwest Russia) under influence of glacial moraine deposits. *Chemical Geology*, 2019, 509, pp.115 - 133. 10.1016/j.chemgeo.2018.12.033 . hal-03485900

HAL Id: hal-03485900

<https://hal.science/hal-03485900>

Submitted on 20 Dec 2021

HAL is a multi-disciplinary open access archive for the deposit and dissemination of scientific research documents, whether they are published or not. The documents may come from teaching and research institutions in France or abroad, or from public or private research centers.

L'archive ouverte pluridisciplinaire **HAL**, est destinée au dépôt et à la diffusion de documents scientifiques de niveau recherche, publiés ou non, émanant des établissements d'enseignement et de recherche français ou étrangers, des laboratoires publics ou privés.



Distributed under a Creative Commons Attribution - NonCommercial 4.0 International License

1
2
3
4
5
6
7
8
9
10
11
12
13
14
15
16
17
18
19
20
21
22
23
24
25
26
27

Chemical weathering of mafic rocks in boreal subarctic environment (northwest Russia) under influence of glacial moraine deposits

Ekaterina V. Vasyukova^{1#}, Priscia Oliva¹, Jerome Viers¹, Francois Martin¹, Bernard Dupré¹,
Oleg S. Pokrovsky^{1,2,3*}

¹*Geoscience and Environment Toulouse (GET, UMR 5563), University of Toulouse, OMP-
CNRS; 14, avenue Edouard Belin, 31400 Toulouse, France*

²*N. Laverov Federal Center for Integrated Arctic Research, Russian Academy of Science,
Nab. Severnoy Dviny 23, 163000 Arkhangelsk, Russia,*

³*BIO-GEO-CLIM Laboratory, Tomsk State University, 36 Lenina, 634050 Tomsk, Russia*

* *Corresponding author email: oleg.pokrovsky@get.omp.eu*

present address: WTE Wassertechnik GmbH, Ruhrallee 185, 45136 Essen, Germany

Keywords: chemical weathering, mafic rocks, soil, fresh waters, boreal zone.

Submitted to *Chemical Geology*, after revision, 24 December 2018

28 **Abstract**

29
30 Chemical weathering of mafic rocks represents substantial sink of atmospheric CO₂
31 yet the mechanisms of this process in high-latitude regions are poorly understood. This work
32 addresses geochemical migration and partitioning of major and trace elements between rock,
33 soil and surface waters during chemical weathering of mafic rocks and soil formation under
34 the influence of a glacial moraine in the northwestern Russian subarctic. We used
35 multidisciplinary approach which included major and trace element chemical analysis, Sr
36 isotopic measurements, and mineralogical structural and microscopic investigations.
37 Quaternary (Pleistocene) deposits were observed even in the deepest horizons of soil profiles
38 and confirm a strong moraine influence as most soils showed podzolic features. Chemical and
39 Sr isotopic analyses revealed a strong impact of the moraine on soil chemistry and
40 mineralogy. Mineralogical studies showed the presence of non-aeolian quartz and zircon in
41 soils which were not linked to the nature of the parental rocks (i. e. mafic and felsic). At the
42 same time, we observed the presence of etch pit corrosion on the surface of zircons and
43 feldspars, and a newly-formed matter adjacent to the surface of primary phases. The chemical
44 index of alteration (CIA) showed weak or no weathering of rocks within the soil profile and
45 the weathering intensity scale confirmed the “felsic” chemical composition of soils developed
46 over mafic and ultramafic rocks. Analysis of Sr radiogenic isotopes demonstrated preferential
47 removal of easily weatherable and less radiogenic minerals over the full depth of soil profile
48 and a more radiogenic signature of the granitic moraine compared to mafic and felsic
49 bedrocks. The composition of most surface waters reflected the weathering of silicate rocks
50 but did not allow for distinguishing purely mafic source. The chemical weathering rates of
51 ultramafic rocks were calculated to be higher than those for the granitic till, but the moraine
52 depositions which dominate this region hide evidence of the real weathering process. This
53 could be due to retention of Mg and Ca in soil due to precipitation of secondary phases such

54 as Mg-vermiculite or divalent cation adsorption on mineral, organic or organo-mineral phases.
55 As a result, weathering rates estimated for the olivinite rock appear to be lower than the
56 weathering rates of mafic rocks reported in other boreal and subarctic regions. Overall, the
57 felsic moraine deposits are capable to sizably decrease the weathering intensity of mafic rocks
58 which should be taken into account for chemical weathering modelling of high-latitude
59 regions subjected to glaciation in the past.

60

61 **1. Introduction**

62 Numerous works have emphasized the significant role of silicate weathering in
63 atmospheric CO₂ consumption and climate regulation; it is considered to be the principal
64 process for removing carbon dioxide from the atmosphere on a long-term scale (Berner et al.,
65 1992, 1995; Boeglin and Probst, 1998; Berner and Caldeira, 1999; Gaillardet et al., 1999;
66 Kump et al., 2000; Dupré et al., 2003). Weathering of continental basalts, accounting for
67 about 30 % of total CO₂ consumption by silicate weathering (Dessert et al., 2003), has been
68 extensively addressed (Gislason et al., 1996; Louvat and Allègre, 1997, 1998; Dessert et al.,
69 2001; Grard et al., 2005; Pokrovsky et al., 2005, Schopka et al., 2011; Gaillardet et al.; 2011,
70 Schoppa and Derry, 2012; Eiriksdottir et al., 2013, 2015; Balagizi et al., 2015; Dessert et al,
71 2015; Ibarra et al., 2016). Recently, it has been shown that the weathering of silicate and
72 carbonate rocks in the Baltic Sea catchment accounts for 3 to 30% of the net ecosystem C
73 exchange, implying that weathering represents a significant sink of atmospheric CO₂ (Sun et
74 al., 2017). In contrast, very few investigations dealt with the impact of chemical weathering
75 on soil formation and CO₂ consumption in the environment underlain by intrusive mafic rocks
76 such as gabbros and olivinite (Schroeder et al., 2000). There are relatively few studies on
77 comparative weathering intensity of acidic versus basic silicate rocks at the catchment scale
78 (Horton et al., 1999; Ibarra et al., 2016; Wymore et al., 2017). Notably, in the Karelia and

79 Kola provinces (northwestern Russia, see **Fig. 1**), cationic weathering fluxes estimated from
80 river water chemical compositions and daily discharges are among the lowest in the world:
81 TDS_c = 0.33 and 2.3 t/km²/yr for granite and basaltic watersheds respectively (Zakharova et
82 al., 2007). Surprisingly for mafic rock dominated watersheds, the Baltic Shield values are
83 only half the value measured for central Siberian basalt (~5 t/km²/yr, Pokrovsky et al., 2005)
84 despite similar runoff but sizeable mean annual air temperature (MAAT) differences
85 (+1 ± 2°C in Karelia versus -9 ± 2°C in Central Siberia). Such a disagreement does not allow
86 reliable extrapolation of the widely used “temperature-basic rocks weathering intensity”
87 relationship (Dessert et al., 2003) for specific subarctic environments in the present and past.
88 Further, the temperature sensitivity of chemical weathering is recognized to be strongly
89 limited by river discharge and water residence time in soils (i.e., Maher, 2011; Maher and
90 Chamberlain, 2014; Ibarra et al., 2016; Raymond, 2017 and references therein). Therefore,
91 studying the weathering mechanisms at the soil and small catchment scales is necessary to
92 explain the differences in mafic rock weathering in Europe and Siberia and to reveal the
93 factors responsible for slower weathering rates under specific environmental conditions
94 present in NW Russia. Recently, strong interest to chemical weathering linked to widespread
95 deglaciation processes (i.e., Foster and Vance, 2006; Stroeven et al., 2016) has been focused
96 around Greenland Ice Sheets (Andrews et al., 2014; Hindshaw et al., 2014; Deuerling et al.,
97 2018), Arctic Islands (Hindshaw et al., 2016), and Iceland (Opfergelt et al., 2014; Hawley et
98 al., 2017).

99 In contrast to the western European boreal environments located in the vicinity of the
100 Baltic Sea that are housed in a relatively mild climate, the understanding of the geochemistry
101 of ecosystems situated along the Arctic sea coast, including the White Sea, still remains quite
102 poor. The Karelia and Kola provinces (northwestern Russia) belong to this zone and offer
103 possibility to study the weathering of the coexisting mafic (e. g. olivinite, gabbro-norite) and

104 felsic (e. g. gneiss, granite) rocks within a relatively small and therefore easily accessible
105 spatial scale. The region is characterised by the presence of abundant glacial moraine and till
106 deposits. In Finland, different genetic moraine types (e. g. ground moraine, Rogen moraine,
107 Pulju moraine, Sevetti moraine, Kianta moraine, De Geer moraine, etc.) were determined
108 according to the classification given by Hättestrand (1997) and their geochemistry,
109 mineralogy and morphology were extensively studied (e.g., Peuraniemi, 1982; Zilliacus,
110 1989; Peuraniemi et al., 1997; Sarala, 2005, Lunkka et al., 2013). The chemical and
111 mineralogical composition of the moraine that covers the study area (northern and southern
112 Karelia) suggest it was formed from Quaternary deposits of Pleistocene age (Evdokimova,
113 1957; State Geological Map of Russian Federation, 2001). Soil ages in this zone are supposed
114 to be around 10 Ky. According to Thiede et al. (2001), Karelia and the Arkhangelsk regions
115 were covered in ice sheets only during the late Weichselian glaciation phase (i. e. 17-15 Ky).
116 Supposedly, during this period the soil erosion process was so important that almost all the
117 soil cover disappeared in contrast to more southern regions (Salminen et al., 2008) where soil
118 profile ages vary from 60 to 150 Ky.

119 Cool and humid boreal regions of Europe are dominated by podzolic soils extensively
120 described in Russia (Dokuchaev, 1880; Ponomareva, 1964) and western Europe (e.g., Muir,
121 1961; Anderson et al., 1982; Buurman, 1984; Righi and Chauvel, 1987; Lundström, 1993;
122 Courchesne and Hendershot, 1997, van Breemen and Buurman, 1998; Lundström et al., 2000,
123 2000a; Buurman and Jongmans, 2005). Podzols are typically found on coarsely textured
124 base-poor parent materials such as sands and sandy tills, and are often located in Precambrian
125 Shield granitic/gneissic environments (Lundström et al., 2000). However, podzol type soils
126 were also described in mafic and ultramafic environment under boreal climate (e. g. Lesovaya
127 et al., 2008; Salminen et al., 2008). The occurrence of podzol type soils over mafic rocks is
128 also suggested in the World Reference Base for soil Resources (IUSS Working Group WRB,

129 FAO, 2006); however, considering the most used taxonomic systems criteria, only few of
130 those podzol type soils which developed over mafic rock could be classified as a true podzol.
131 Indeed, even if soils show a podzol like morphology (i. e. occurrence of an eluvial “albic”
132 horizon overlying a reddish-brown illuvial “spodic” horizon), the pH of these soils are usually
133 too high compared to classic podzols (D’Amico et al., 2008). According to D’Amico et al., in
134 such a case, the podzolisation process is favoured by the occurrence of quartz-rich
135 allochthonous material such as aeolian deposit or till. The question of the role of moraine
136 deposits in boreal podzol pedogenesis under a granitic environment was also raised by a
137 number of recent works devoted to the study of mineralogical and major and trace element
138 composition (as well as calculation of weathering losses) of podzols and spodosols developed
139 on granite-gneiss glacial moraine deposits in northern Europe (Öhlander et al., 1991, 1996,
140 2003; Giesler et al., 2000; Melkerud et al., 2000; Olsson and Melkerud, 1989, 2000; Land and
141 Öhlander, 2000; Land et al., 1999, 1999a, 2002; Tyler, 2004; Starr and Lindroos, 2006).
142 Lundström et al. (2000a) reported results of a multidisciplinary study (combining
143 geochemical, mineralogical, micromorphological, microbiological, hydrochemical and
144 hydrological investigations) aimed at testing various mechanisms (adsorption/precipitation
145 versus biodegradation) controlling the formation of podzols in glacial till context. Clay
146 mineralogy and chemical weathering of soils in a recently deglaciated arctic-alpine
147 environment in Sweden were studied by Allen et al. (2001). The authors suggest that the
148 occurrence of mixed layer minerals could be a tracer of parental rock weathering in soils
149 affected by moraine deposits. Contrastingly, Akselsson et al. (2006) found that there is no
150 relation between elemental content and mineralogy of till and bedrock mineralogy for
151 podzolic soil in southern Sweden and concluded that the information on the bedrock is not
152 sufficient for prediction of till mineralogy.

153 In northwestern Russia chemical and mineralogical composition of soils developed on
154 nepheline syenite, amphibolite and metamorphized diabase that were affected by moraine
155 deposition were recently studied by Lesovaya et al. (2008). These authors argued that soil
156 profiles became thicker and showed notable clay mineral transformation when allochthonous
157 moraine material is intermixed. In a more recent study (Lesovaya et al., 2012), the same team
158 studied chemical weathering processes of mafic rocks in the polar Ural and emphasised
159 weathering of smectite and secondary iron hydroxide accumulation in relation with
160 acidification processes (biota effect) which are unusual in ultramafic environment. Thus,
161 despite these aforementioned studies on soil formation and chemical weathering processes in
162 boreal environment, there is still a lack of studies devoted to soil forming processes on mafic
163 rocks and related river hydrochemistry under glacial moraines.

164 Towards improving our understanding of mafic rocks weathering in boreal climate, we
165 use a multidisciplinary approach which is comprised of studying the geochemical migration
166 and partitioning of major and trace elements between different reservoirs (rocks and soils),
167 major and trace elements analysis, Sr and Nd isotopic measurement, and mineralogical
168 investigation. We aimed at characterizing rock weathering rates and adjacent rivers
169 hydrochemistry in order to understand the soil forming processes on basaltic rocks in the
170 boreal zone influenced by glacial moraine.

171 For this, we studied mafic and felsic rocks, as well as soil and water samples collected
172 within the Kivakka (northern Karelia) and Vetreny Belt (southeastern Karelia) magmatic
173 formations that are bounded by Archean age crystalline granitic rocks. The main questions we
174 attempt to answer in this study are: *i*) “to what degree the presence of a granitic-gneissic
175 moraine can modify the weathering features of basic rocks and degree of element leaching
176 from these rocks?”, *ii*) “what are the differences between different mafic rock (gabbro,
177 norites, peridotites, olivinites, and basalts) degree of alteration in soils under the same

178 environmental conditions (climate, vegetation)?” and *iii*) “how contemporary weathering
179 processes are reflected in surface and soil water chemical compositions?”

180

181 **2. Geological and geographical setting**

182 The Vetreny Belt paleorift and the Kivakka layered intrusion are situated in the
183 Karelian region of northwestern Russia and exhibit similar geological, climatic, and
184 hydrological conditions. The main difference between these two sites is the nature of their
185 mafic rocks: gabbro-norite (peridotite) create the Kivakka intrusion and basalts with some
186 olivinites create the Vetreny Belt.

187

188 *2.1. Lithology, soils and vegetation*

189 The Karelian region is situated in the north-western part of Russia, bordering Finland
190 to the west, Lakes Ladoga and Onega to the south, and the White Sea – an extensive gulf of
191 the Arctic Ocean – to the east. Largely a hilly plain, the region has mountains in the west with
192 elevations up to 600 m. The lowest elevations are near the White Sea and the many lakes that
193 have filled depressions scoured across the surface during the last glaciation period. The relief
194 of Karelian zone was formed under the influence of glaciation which occurred at least 3 times
195 during Pleistocene (Reimann and Melezhik, 2001) with and the last glacier disappearing about
196 20-10 thousand years ago.

197 The study area is also a part of the Eastern Fennoscandian Shield. A simplified map of
198 the two chosen sites along with sampling points and some geological information are given in
199 **Fig. 1.** Quaternary deposits consist primarily of coarse-grained and sandy till or glaciofluvial
200 deposits showing well-developed podzol profiles. Detailed information of major and trace
201 element composition of volcanic rocks and rock-forming minerals utilized in this work can be
202 found elsewhere (Amelin and Semenov, 1996; Koptev-Dvornikov et al., 2001; Bychkova,

203 2003; Bychkova and Koptev-Dvornikov, 2004; Bychkova et al., 2007 for the Kivakka layered
204 intrusion; Kulikova and Kulikov, 1981; Ryabchikov, 1988; Puchtel et al., 1996, 1997;
205 Kulikov, 1999; Kulikov et al., 2005 for the Vetreny Belt; Lobach-Zhuchenko et al., 1986,
206 1993; and Bibikova et al., 2005 for the Archaean granitic and tonalitic gneisses surrounding
207 the chosen intrusions).

208 The main part of the studied zone belongs to a boreal taiga forest ecosystem with pine,
209 fir, birch, ericaceous species, and mosses that cover more than 80 % of the territory.
210 Approximately 20 % of the territory is covered by wetlands that were developed on thick peat
211 and gley-podzol soils. On well-drained territories alluvial-ferruginous-humic and alluvial-
212 humic podzols prevail. They are developed under pine- and spruce-pine forests with moss-
213 fruticulose cover. The soil depths in the region vary from 30-40 cm in the northern part and
214 60-85 cm in the southern part of Karelia. On the hill tops (100-200 m) soil depths do not
215 exceed 10-20 cm. Ferruginous podzols are remarkable for high acidity, especially in
216 superficial horizons (Lundström et al., 2000a and references therein). Soils are partly
217 developed on a glacial granite moraine which consists mainly of sand and loamy sand with
218 gravel and boulder inclusions. The glacio-lacustrine and lacustrine as well as fluvio-glacial
219 deposits commonly form in lenses and are wide spread (Zakharova et al., 2007).

220

221 2.1.1. *Vetreny Belt paleorift*

222 The Vetreny Belt (63°46'N – 35°48'E) (**Fig. 1**, left) is situated in the south-eastern
223 part of the Baltic Shield on the territory of the south-eastern Karelia and Arkhangelsk regions.
224 It occupies a territory of approximately 5200 km² and can be traced from Lake Vyg
225 southeastward over a distance of more than 250 km. Its width increases from 15 to 85 km to
226 southeastward where it plunges beneath Paleozoic cover of the Russian platform and extends
227 further southeast (Kulikov et al., 2003). A detailed description of the Vetreny Belt suite is

228 given by Puchtel et al. (1997) who also suggested that massifs like Kivakka layered intrusion
229 have an origin related to the Vetreny Belt volcanic and plutonic rocks. The Vetreny suite
230 consists entirely of a thick unit of basaltic komatiites belonging to the Sumian and younger
231 groups in the area (Kulikov and Kulikova, 1982). The isotopic dating of the Vetreny belt
232 yielded the following ages: 2449 ± 35 Ma and 2410 ± 34 Ma (Sm-Nd), 2424 ± 178 Ma (Pb-
233 Pb), 2437 ± 4 Ma (U-Pb) (Puchtel et al., 1997).

234

235 *2.1.2. Kivakka layered intrusion*

236 The Kivakka pluton ($66^{\circ}12'N - 30^{\circ}33'E$) (**Fig. 1**, right) is located in northern Karelia
237 and belongs to a complex of layered peridotite-gabbro-norite intrusions in the Olanga group
238 that hosts migmatized biotite and amphibole gneisses, granite-gneisses, and granodiorite-
239 gneisses of Late Archean age (Lavrov, 1979; Amelin et al., 1995). In addition to the Kivakka
240 pluton, the group includes the Lukkulaivaara and Tsipringa massifs (Shmygalev, 1968;
241 Lavrov, 1979; Klyunin et al., 1994; Semenov et al., 1995; Amelin and Semenov, 1996). All
242 of these are spatially restricted to an east-west trending regional fault zone and comprise the
243 eastern branch of an extensive belt of layered massifs whose western branches continue across
244 Finland (Alapieti, 1982). Detailed geological and petrological descriptions of the Kivakka
245 layered intrusion can be found in the work of Koptev-Dvornikov (2001). The isotopic dating
246 of the massif yielded the following ages: 2420 ± 23 Ma (Sm-Nd), 2445 ± 3.4 Ma (Zr) and
247 2444 ± 1 Ma and 2445 ± 2 Ma (Amelin and Semenov, 1990, 1996; Barkov et al., 1991;
248 Balashov et al., 1993).

249

250 *2.2. Climate and hydrology*

251 The climate of most of the territory is mildly cold, transitioning between oceanic and
252 continental, with a dominant influence of the Arctic and Northern Atlantics. Snow period lasts

253 from October through April-May with snow cover thickness ranging from 70 up to 110 cm.
254 Mean annual temperature is close to 0°C but extremes can reach as high as +35° and as low as
255 -35°C in summer and winter periods, respectively. Mean precipitation amount is between 400
256 and 600 mm/yr.

257 The region has a well-developed river network that flows via a system of glacial lakes.
258 Chemical composition of river water in Karelia is determined by chemical weathering of
259 silicate parent rocks of the Baltic crystalline shield, quaternary deposits, and the presence of
260 numerous peatlands. Typical values of total dissolved solids (TDS) for this region are 15-
261 30 mg/l (Maksimova, 1967; Zakharova et al., 2007) and the concentration of suspended
262 matter in the river is very low. The study region can be considered as pristine, although some
263 influence from Kola peninsula smelters can be pronounced via long-range atmospheric
264 pollution (i. e. de Caritat et al., 2001).

265

266 **3. Materials and methods**

267 *3.1. Sampling of rocks, soils, surface waters and soil pore waters*

268 A list of soil, water, and soil water samples as well as their bedrock composition is
269 presented in **Table 1**. For both soils and waters, series named “V” and “K” correspond to
270 samples collected within the Vetreny Belt paleorift or Kivakka layered intrusion zones,
271 respectively. Three altered rocks – an Archean gneiss, basalt, and peridotite – were sampled
272 within the Vetreny Belt intrusion zone while two other basic rocks – a gabbro-norite and
273 olivinite – were sampled from Kivakka layered intrusion in order to investigate formation of
274 secondary phase minerals in thin sections. Ten soil profiles, five from each study site and five
275 from each type of mafic and felsic parent rocks were sampled for pedological, mineralogical
276 and chemical analysis (see **Table 1** for description and **Table SI-1** of **Supplementary**
277 **Information 1** for chemical composition of soils).

278 Small and large rivers, as well as several wetlands and soil pore waters draining
279 through mafic and felsic rocks were sampled during extensive field campaigns in July 2004
280 and July 2006 for dissolved major and trace elements contents. Each location was sampled
281 only once. Three types of water were chosen for this study: river water, bog water, and
282 interstitial soil solutions draining from both felsic and mafic rocks (see **Table 1** for
283 description and **Table 2** for chemical composition of waters).

284

285 *3.2. Analytical techniques*

286 *3.2.1. Mineralogical and chemical analysis of rocks and soils*

287 Mineralogical studies on altered rock material were made on polished consolidated
288 thin sections using optical microscopy, scanning electron microscopy (SEM GEOL 6360LV
289 coupled to EDS PGT SDD SAHARA) including X-ray microanalysis, and electron
290 microprobe analysis (CAMECA SX50) in the GET laboratory (Toulouse). Modal composition
291 of the different altered rock samples was calculated by using structural formulae of minerals
292 and chemical composition of parental rocks and was coupled with SEM information. Analysis
293 of clays in soil sample K-14 (C horizon) was performed by transmission electron microscopy
294 (TEM) in the CRMCN laboratory, Paul Cézanne University, Aix-Marseille III, France.

295 The individual composition of soil minerals was determined by SEM with EDS on soil
296 grain thin sections. Afterwards, a structural X-ray diffraction analysis (XRD) was performed
297 on soil clay fractions in the GET laboratory (Toulouse). Clay fraction (i. e. < 2 μm grain size)
298 was separated by decantation in water column. Furthermore, structural XRD analysis
299 performed on INEL G3000 Cu $K\alpha_{1,2}$, oriented samples were prepared by dropping of
300 < 2 μm suspension on a glass plate and drying it at room temperature. Standard treatment
301 (H_2O , ethylene glycol, and heating at 500°C) was employed to assess the interlayer distances
302 of clay minerals.

303 After crushing, pulverization, and homogenization, soil samples were digested in H₂O₂
304 at 25°C for 24 h and then in HF-HNO₃-HCl on a hot plate at 60-120°C in Teflon beakers in a
305 clean room (classes between 5 and 7 according to the ISO 14644-1 standard). The validity of
306 total chemical analysis for soils was verified by applying the same procedure for international
307 geostandards BE-N (i. e. basalt), GA and AC-E (i. e. granites) for rocks, and LKSD-1 (i. e.
308 lake sediment) for soils. Trace elements in rocks and soils were analysed by ICP-MS with an
309 uncertainty < 10 % for the elements presented in this study. Indium and rhenium were used as
310 internal standards. Major elements in soils were analysed by ICP-AES method in SARM
311 laboratory (Nancy, France) and ALS Chemex laboratory (Vancouver, Canada). The analytical
312 error of these measurements was in the range 5-10 %.

313 Total organic carbon (TOC) was analysed in dried soils by a Horiba carbon/sulphur
314 analyzer EMIA-320V with an uncertainty better than 10 %. Soil pH was measured in
315 deionised water suspension according to international ISO norms for measuring soil pH
316 (AFNOR, 1996, ISO 10 390). The accuracy of measurements was ± 0.05 pH units.

317

318 *3.2.2. Chemical analysis of river, mire and soil pore waters*

319 Physico-chemical parameters of unfiltered water samples (pH, temperature (± 0.2°C),
320 and electrical conductivity) were measured in the field. The pH was measured using a
321 combined Schott-Geräte electrode calibrated against NIST buffer solutions (pH = 4.00 and
322 6.86 at 25°C), with an accuracy of ± 0.02 pH units. Samples were collected from near the
323 middle of the flow channel, using 1-l high-density polyethylene (HDPE) containers held out
324 from the beach on a non-metallic stick. Vinyl gloves were always used during handling of the
325 samples. The water samples were immediately filtered through sterile, single-use Minisart®
326 filter units (Sartorius, acetate cellulose filter) with pore sizes of 0.45 µm. The first 200 ml of
327 the filtrate were systematically discarded. Filtered solutions for cations, trace element and Sr

328 isotope analyses were acidified (pH = 2) with ultrapure double-distilled HNO₃ and stored in
329 HDPE bottles previously washed with ultrapure 0.1 M HCl and rinsed with MilliQ deionized
330 water. Filtered water samples for anions were not acidified and stored in HDPE bottles
331 previously washed according to the above-described procedure for cations. Samples for
332 dissolved organic carbon (DOC) were collected in pyrolysed (550°C) Pyrex test tubes.

333 Soil pore waters were extracted from humid soil horizons in the field using a Ti
334 pressure device. This titanium vessel has a 50 mm diameter, 150 mm length, and a special
335 thread allowing it to reach 20 000 kg/cm² pressure. Depending on saturation state of soil
336 samples, 10 to 50 ml of solution was collected and filtered through a 0.45 µm filter. After
337 each extraction, the vessel and its compartments were thoroughly washed with river water,
338 and afterward, by 100 to 200 ml with distilled water. Before and after fieldwork, blank
339 samples were run by filling the pressure system with MilliQ water at neutral pH and letting it
340 to react for 24 h. No detectable contamination of major and trace elements and DOC was
341 observed.

342 Major anion concentrations (Cl, SO₄, F, NO₃, PO₄) were measured by ion
343 chromatography (HPLC, Dionex ICS 2000) with an uncertainty of 2 %. Calcium, magnesium,
344 sodium, and potassium concentrations were determined using an atomic absorption
345 spectrophotometry (AAS) Perkin-Elmer 5100PC spectrometer with an uncertainty of 2 %.
346 Aqueous silica concentration was determined by standard colorimetry (molybdate blue
347 method) with an uncertainty of 2 % using Technicon automated analyzer. Alkalinity was
348 measured by potentiometric titration with HCl to pH = 4.2 using Gran method with detection
349 limit of 10⁻⁵ M and an uncertainty of 2 %. DOC was analyzed using a Carbon Total Analyzer
350 (Shimadzu TOC 5000A) with a detection limit of 0.1 µg/l and an uncertainty better than 3 %.

351 Trace elements were measured without preconcentration by ICP-MS (Elan 6000,
352 Perkin Elmer and 7500ce, Agilent Technologies). Indium and rhenium were used as internal

353 standards. The international geostandard SLRS-4 (Riverine Water Reference Material for
354 Trace Metals certified by the National Research Council of Canada) was used to check the
355 validity and reproducibility of each analysis. A good agreement between our replicated
356 measurements of SLRS-4 and the certified values was obtained (relative difference < 5 %).

357

358 *3.2.3. Isotope analysis of surface waters and soils*

359 Strontium and neodymium isotopic ratios were measured by thermal ionization mass
360 spectrometry (TIMS) (Finnigan Mat 261) preceded by chemical separation, involving the
361 dissolution of the sample and chemical extraction of Rb, Sr, Sm and Nd by ion exchange
362 chromatography using three chromatographic materials Sr.Spec, TRU.Spec and Ln.Spec, and
363 HF, HNO₃ and HCl acids in a clean room. Data correction was based on the systematic
364 analysis of the NBS 987 standard for Sr and the La Jolla standard for Nd (i.e., correction for
365 instrumental mass fractionation based on hourly drift at the day of analyses). During this
366 work, the average ⁸⁷Sr/⁸⁶Sr for NBS 987 standard was 0.710250 ± 0.000010 (4 measurements)
367 and 0.511834 ± 0.000006 for ¹⁴³Nd/¹⁴⁴Nd (1 measurement).

368

369 **4. Results**

370 *4.1. Bedrock and soil mineralogy and chemistry*

371 The mineralogy and chemistry of studied rocks are described in **Supplementary**
372 **Information 2**. Mineral composition of solid material was characterized by structural X-ray
373 analyses of fine (< 0.1 μm, 0.1-2 μm and > 2 μm) and bulk fractions of 10 soil profiles:
374 samples V-4, V-7 (basalts), V-9, V-16 (gneisses), V-15 (peridotites, olivinites) and K-7, K-29
375 (gneisses), K-14 (olivinites), K-37 (gabbro-norites). Clay mineralogy results presented in this
376 study were obtained on soil samples having enough fine fraction for analysis. However, in
377 boreal podzols, the clay fraction is generally known to be < 5 % (Melkerud et al., 2000;

378 Mokma et al, 2004; Allen et al., 2001). Although peak intensities in the diffractograms varied
379 somewhat as a function of depth, the $< 2 \mu\text{m}$ fractions from soils developed on basic rocks
380 indicated that quartz (all samples except K-14-C and V-15-O/A), feldspar (all samples except
381 K-14-B₁ and -C and V-15-O/A), amphibole (all samples except K-14-B₁), illite (all samples),
382 chlorite (all samples except K-37-A, V-16-E and -B, V-9-A and V-15-O/A), vermiculite (K-7,
383 K-14, K-37-B₁ and -B₂, V-16-B, V-15), as well as interstratified layers illite/vermiculite
384 (K29-O/A), smectite (K-37-B₁, V-4-E and V-15-O/A) and amorphous phases (K-29, V-16, V-
385 7 and V-9) were the major clay-fraction constituents (**Table 3**). Amorphous aluminosilicates
386 (i. e. imogolite), chlorite, regular interstratified layer mica/vermiculite (25 Å) were found in
387 soil profile K-29 developed on granite-gneiss which is comparable to the clay fraction
388 composition of podzols developed on granite-gneissic rocks in southern Sweden described by
389 Schweda et al. (1991) and in northern Sweden described by Land et al. (1999). Hydrobiotite, a
390 mineral containing regularly interstratified layers of biotite and vermiculite (Sawhney, 1989,
391 Murashkina et al., 2007), was indicated by a peak at 12 Å in felsic soil K-29.

392 The analysis of the clay fraction in K-14 (**Fig. 2**) indicated the presence of vermiculite
393 (occurrence of a 14.4 Å (7.3 Å) peak on the air-dried pattern, expandable on the ethylene-
394 glycol pattern and collapsed on the heated pattern), illite (10 Å) and amphibole (8.4 Å). The
395 analysis of V-15 peridotite (**Fig. 2A**) showed the presence of both of expandable vermiculite
396 and smectite (vermiculite predominant), and an interstratified layer of illite/vermiculite
397 (23.4 Å). The TEM investigations on the K-14 sample over olivinite from the Kivakka
398 intrusion allowed for acquisition of detailed information on the nature of vermiculite formed
399 in the C horizon of this soil (**Fig. 2B**). These results confirmed the presence of Mg-
400 vermiculite together with chlorite and amphibole which also contained Mg.

401 Optical and SEM observations on consolidated thin sections of structurally preserved
402 soil samples from different horizons revealed the presence of quartz and feldspar in almost all

403 studied soil profiles developed on basic rocks: gabbro-norite, olivinite, and peridotite, with the
404 exception of the C horizon of K-14 (soil over olivinite) and the O/A horizon of V-15 (soil
405 over basalt). Zircon was found in soils developed on granite-gneisses (K-7, B horizon; K-29,
406 C horizon, V-16, E horizon). Morphological observations of soils by SEM carried out during
407 this study reveal the presence of etch pits corrosion on the surface of zircon and feldspar
408 (**Fig. 3 A, B**) together with newly-formed matter visible as a coating on quartz, plagioclase
409 and pyroxene surfaces (**Fig. 3 C**). The pH (H₂O) of soils developed on felsic rocks varied
410 between 3.43 and 7.60, and those on basic rocks between 3.82 and 8.74, being the most acid
411 in the surface organic rich soil horizons. The high pH found for V-4 and K-14 soils could be
412 attributed to the mafic nature of the parental rock. Podzolisation process is favoured within
413 low pH environment which is usually the consequence of pedogenesis on acid rocks under
414 deep and acid litter. In this context, the pH (H₂O) measured for the V-16-B and K-8-B
415 samples are problematic (pH is too basic for a podzol type soil). The TOC concentration
416 ranged from 7.7 to 42.1 % wt in organic surface horizons (O/A), and from 0.15 to 3.5 % wt
417 for deeper horizons (E, B and C).

418 Chemical analysis of soils was performed on bulk fractions (including gravel).
419 Observations of elements concentrations along the soil profiles (not shown) show that all soils
420 developed on felsic rocks exhibited higher content in Si, K (except K-29), Al (except K-7)
421 and Na, and lower content in Ca (except K-29), Fe and Mg with respect to their parent rock.
422 Podzol V-7 developed on basic rocks showed relatively higher content in Si, Al, Na and K
423 than its parent rock similarly to the soils developed on felsic rocks (V-9, K-8, K-29). K-14
424 and K-37 exhibit low Si, Al and Na content compared to olivinite or gabbro-norite. Higher
425 content in K in the surface horizon compared to the parental rock was observed for all soils
426 except K-14, K-29 and V-15. Almost all soils developed on basic rocks showed lower content
427 in Fe (except K-14) and Mg (except V-9 and V-15) compared to their respective parent rock.

428 Photos of podzols V-4, K-14 and K-37 developed on basalt, olivinite and gabbro-
429 norite, respectively, and regosol K-29 over gneiss are presented in **Fig. 4**. A diagram of
430 weathering intensity scale (WIS) used to evaluate the chemical index of alteration (Meunier et
431 al., 2013) allows to see how the moraine influences the chemistry of soils (**Fig. 5**). Regardless
432 of the parent rock, the majority of soil samples are located in the “felsic” domain.

433

434 *4.2. REE distribution pattern*

435 The upper crust (Taylor and McLennan, 1985) normalized rare earth elements (REE)
436 patterns for selected soil samples are plotted in **Fig. 6**. REE patterns of soil horizons are
437 different from those of the corresponding parent rocks. A slightly positive europium anomaly
438 can be observed in the majority of soil horizons and is likely to be related to the presence of
439 feldspar in the soil-rock system. Eu/Eu^* (**Table SI-1**) is calculated using the formula (Condie,
440 1993):

$$441 \quad Eu/Eu^* = Eu_N / (Sm_N \cdot Gd_N)^{1/2}$$

442 where $Gd = (Sm \cdot Tb^2)^{1/3}$. The ratio is within the range 0.87-1.05 for soils on basic rocks for
443 both the Vetreny Belt and the Kivakka intrusion, and 0.88-1.18 and 0.91-1.09 for soils on
444 felsic rocks for the Vetreny Belt and the Kivakka intrusion, respectively. It can be observed
445 that the ratios are quite similar for both felsic and mafic soil-rock systems, again confirming
446 the influence of exterior moraine deposits. This result is further corroborated by extended
447 upper crust (UC) normalized diagrams that include all major and trace elements (**Fig. 7**). The
448 soils of felsic and mafic origin from the Kivakka intrusion site (samples K-7, K-8, K-29 and
449 K-37) are shown in **Fig. 7 A** and for soils from the Vetreny Belt site (samples V-7, V-9, V-16,
450 V-4 and V-15) are shown in **Fig. 7 B**. It can be seen that all soils from the Kivakka intrusion
451 zone exhibited quite similar upper-crust normalized trace elements patterns independent on
452 their parent rock. The soils were generally depleted in most elements compared to the upper

453 crust: Li, Sc, Mn, Co, Ni, Cu, Zn, As, Rb, Y, Zr, Nb, Mo, Cd (except surface horizons O/A of
454 soils K-7, K-29 and K-37), Sb, Cs, Hf, Ta, W, Tl, Pb, Th, U. For these elements surface
455 horizons O/A appear to be more depleted than the deeper ones. Olivinitic soil K-14 (not
456 shown) exhibited a slightly different pattern, being less depleted in the above mentioned
457 elements relative to the upper crust and enriched in Cr, Co, Zn and Ni, in accord with these
458 elements elevated concentration in the source rocks. For some soil samples a slight
459 enrichment in V (samples K-7-B, V-9-A, V-15-O/A), Cr (K-37 all horizons, V-15-O/A
460 (significantly enriched), V-9-A, V-7-B), Sr (K-29, E and C horizons), Cd (K-7-O/A, K-37-O,
461 V-9, O and A horizons, V-7-E) and Sb (K-7-O/A, K-29-O/A, V-9-O) relative to the upper
462 crust can be observed. The last observation is also true for V-15 sample developed on
463 ultramafic rocks. The soils from the Vetreny Belt zone (**Fig. 7 B**) exhibited similar pattern
464 independent on their parent rocks, and most of them are depleted in Sc, Ti, Co, Ni, Cu, Zn,
465 Ge, Rb, Sr, Y, Zr, Nb, Cs, Hf, Ta, Th, U and significantly in Pb compared to the upper crust.
466 The surface horizons O/A were depleted in V, Cd and Sb. A-horizon of soil V-9 and V-15
467 were enriched in Sc, V, Cr, Co, Ni, Cd, and all soils were significantly enriched in Tl with
468 respect to the upper crust. Overall, results on TE partitioning in soils corroborate the previous
469 conclusion on the dominant role of glacial deposits on soil chemistry both on mafic and felsic
470 rocks. Taken together, all soils from the Kivakka intrusion and the Vetreny Belt zone exhibit
471 quite similar UC-normalized trace element patterns independent on their parent rock. This
472 confirms the dominant role of glacial deposits on soil chemistry for both mafic and felsic
473 rocks, i.e., the glacial erosion has predetermined the soil development.

474

475 *4.3. Hydrochemistry of rivers and soil porewaters*

476 Measured pH and temperature, dissolved organic carbon (DOC) concentration, major
477 and some trace elements concentrations (Al, Fe, Sr and Rb), as well as $^{87}\text{Sr}/^{86}\text{Sr}$ isotopic ratios

478 for river and stagnant mire waters are presented in **Table 2** for both the Kivakka intrusion and
479 the Vetreny Belt zones. The studied waters were essentially of neutral pH varying from 6 to
480 7.5. However, some surface organic rich waters and bog waters were more acidic with pH
481 decreasing to 4.5-5.5. Bicarbonate ion concentrations ranged from 1.8 to 40.2 mg/l for rivers
482 draining basic rocks and from 8.3 to 80.2 mg/l for rivers draining felsic rocks. In surface
483 wetlands and interstitial waters from soils developed on basalts, the alkalinity ranged from 2.2
484 to 8.0 and from 1.8 to 29.9 mg/l, respectively. The majority of surficial fluids exhibited high
485 concentrations of dissolved organic carbon between 5 and 40 mg/l.

486 The composition of the dissolved load of most rivers reflects the weathering of silicate
487 rocks because the total dissolved solids (TDS) expressed as a sum of major inorganic species
488 concentrations (Na, Ca, K, Mg, Al, Fe, H₄SiO₄, Cl, NO₃, and SO₄) was low (between 10 and
489 30 mg/l). These measurements are comparable with previous results on Karelia region
490 (Feoksitov, 2004, Zakharova et al., 2007). Rivers analyzed in this study had an average Si
491 concentration of around 4 mg/l (3.6 ± 0.9 and 4.3 ± 1.3 mg/l for rivers draining felsic and
492 mafic rocks, respectively) which constitutes only 30 % of the TDS. Calcium and sodium were
493 dominant among cations in these waters.

494 The concentration of major dissolved cations in surface (river and bog) water for both
495 the Vetreny Belt and the Kivakka intrusion zones (average values in $\mu\text{mol/l}$ are given in
496 brackets) followed the order Ca (336) > Mg (116) > Na (77) > K (16) for waters draining
497 through felsic rocks and Mg (95) > Ca (77) = Na (77) > K (7) for those draining through
498 mafic rocks. Potassium and sodium concentrations (16 $\mu\text{mol/l}$ and 90 $\mu\text{mol/l}$, respectively)
499 were comparable with those reported by Ingri et al. (2005) for a pristine boreal Kalix river
500 draining through a mixed felsic and carbonate-shale environment, whereas calcium content in
501 this study is higher than that of the Kalix river (149 $\mu\text{mol/l}$). We did not detect any systematic
502 difference in Mg concentration between felsic and mafic catchments; concentration varied

503 from 400 to 8000 $\mu\text{g/l}$ within the Vetreny belt zone and from 100 to 13000 $\mu\text{g/l}$ within the
504 Kivakka intrusion zone. Within the basic rocks catchments, we could not detect any sizeable
505 difference between waters draining through rocks of different composition (gabbro-norites,
506 olivinite, and basalts).

507

508 *4.4. Radiogenic isotope features*

509 Concentrations of Rb, Sr, Sm and Nd, and $^{87}\text{Sr}/^{86}\text{Sr}$ and $^{143}\text{Nd}/^{144}\text{Nd}$ isotopic ratios for
510 soils from the Vetreny Belt and the Kivakka intrusion are reported in **Table SI-1**. Peculiar
511 feature of soil and water geochemistry in considered zones is large variation of their Sr
512 isotopic composition (**Fig. 8**). For the Kivakka intrusion, soils developed on olivinite (K-14,
513 the deepest horizon) and TTG (K-29) have lower $^{87}\text{Sr}/^{86}\text{Sr}$ ratios (0.704) similar to parental
514 rock isotope ratios (Amelin and Semenov, 1996). An opposite tendency is obtained for other
515 soils developed on mafic and felsic rocks (**Fig. 8 A**). For example, $^{87}\text{Sr}/^{86}\text{Sr}$ ratios of the
516 samples K-37 (0.721-0.726) which was developed on gabbro-norites are similar to those of
517 felsic K-8 (0.721-0.725). These samples are enriched in Rb, and have the same $^{87}\text{Sr}/^{86}\text{Sr}$ ratio
518 as estimated by Land et al. (2000) for podzols developed on Quaternary till of granitic
519 composition in northern Sweden (0.721-0.727). Furthermore, soil horizons B₂ and C of
520 ultramafic sample K-14, and B₂ of mafic sample K-37 have similar pedological characteristics
521 to those of the B horizon of felsic sample K-7, and quite similar in isotope ratio ($^{87}\text{Sr}/^{86}\text{Sr}$
522 ~ 0.718 and $^{87}\text{Rb}/^{86}\text{Sr} \sim 0.6$). The soils developed on mafic rocks from the Vetreny Belt zone
523 exhibited similar features with $^{87}\text{Sr}/^{86}\text{Sr}$ and $^{87}\text{Rb}/^{86}\text{Sr}$ isotope ratios higher than their source
524 rocks. This unambiguously suggests strong influence of external (moraine) deposits.
525 Concerning the isotopic composition of surface waters, the results demonstrate two similar
526 tendencies for both sites (**Fig. 8 B**): *i*) waters show higher Sr isotopic ratios (between 0.715
527 and 0.730) compared to rocks and rock minerals (between 0.705 and 0.713) within the same

528 range of $^{87}\text{Rb}/^{86}\text{Sr}$ ratios (from 0 to 0.4), and *ii*) Sr isotope ratios of waters are in the same
529 range as soils (except for soil V-15 from Vetreny Belt site) although soils have higher
530 $^{87}\text{Rb}/^{86}\text{Sr}$ ratios (0.3-0.75) than water (< 0.3). Thus, surface waters have a more radiogenic
531 signature than parental rocks and primary minerals for “basic rock derived” samples.

532

533 **5. Discussion**

534 *5.1. Moraine influence over the full depth of soil profile*

535 5.1.1. Major elements

536 The occurrence of corroded zircon and feldspar and the evidence of clay mineral
537 formation in those soils witness similar weathering processes on all types of parental rock.
538 Etch-pitting of zircon is usually related to intense weathering processes, generally in tropical
539 environment (e. g. Oliva et al., 1999). However, the lack of kaolinite neoformation and the
540 persistence of amphibole and plagioclase feldspar in soils suggest not very intense weathering
541 processes, consistent with the beginning of pedogenesis about 10 Ky ago. Our mineralogical
542 observations of secondary phases are consistent with the presence of hydrobiotite, amorphous
543 phases, smectite and K-feldspar over nepheline syenite in horizons C and B₂ as well as quartz
544 and plagioclase in horizons B₁ and E described in mountainous tundra soils of northwestern
545 Russia (Lesovaya et al., 2008). These results are also compatible with the clay fraction
546 composition of soils developed on glacial moraines in Finland (gneissic moraine material)
547 (Melkerud et al., 2000; Mokma et al., 2004) which includes quartz, plagioclase, K-feldspar,
548 amphibole, chlorite, illite, mixed layer illite/vermiculite, and allophanes. Observed mixed
549 layer chlorite/vermiculite is reported as a product of degradation of chlorite.

550 Classically, element depletion or enrichment in soils samples compared to respective
551 unaltered rocks at the soil profile scale (i.e., mass balance approach) is estimated via element
552 ratios with invariant low-mobility elements (i. e. Zr, Ti, Al, Th) in soils and rocks (**Table SI-**

553 1). Theoretical concentrations of major elements in soil profiles were systematically higher
554 compared to the parental rock for Na and/or K except for the B₁ and C-horizons in samples K-
555 14 (soil over olivinite, Kivakka intrusion) and V-15 (soil over peridotite, Vetreny Belt).
556 Moreover, the Zr/Ti ratio was not constant along the soil profiles as we observed a depletion
557 in Zr in O and A horizons and slight enrichment in B horizons. This may suggest that Zr or Ti
558 were not initially homogeneously distributed in soils or that Ti is not invariant in these
559 profiles. Potential Zr mobility in soils and the difficulty of using Zr as refractory element for
560 mass balance calculations are widely known (see recent work in Southern Spain, Ameijeiras-
561 Marino et al., 2017). Similar results were observed when using Al and Th as invariants. One
562 reason for this discrepancy can be the unusually high mobility of tetravalent elements in the
563 form of large-size organo-mineral ferric colloids whose presence is unambiguously
564 demonstrated in surficial waters of the Karelian zone (Pokrovsky and Schott, 2002;
565 Vasyukova et al., 2010). Using a CDF (chemical depletion fraction corresponding to the ratio
566 of chemical erosion rates to mineral supply rates) and chemical depletion fractions of
567 individual elements (Brimhall et al., 2001; Riebe et al., 2001 and 2004; Ferrier et al., 2016)
568 provide a more comprehensive approach of the chemical differentiation of the soil relative to
569 its parent material. In particular, CDF calculations allow to take into consideration external
570 element supply to the soils. Following Riebe et al. (2001, 2004), we calculated:

571
$$\text{CDF} = 1 - ([\text{Ti}]_{\text{rock}} / [\text{Ti}]_{\text{soil}})$$
 for the entire soil

572
$$\text{CDF}_X = 1 - \left(\frac{[\text{X}]_{\text{soil}}}{[\text{X}]_{\text{rock}}} \times \left(\frac{[\text{Ti}]_{\text{rock}}}{[\text{Ti}]_{\text{soil}}} \right) \right)$$
 for individual element X

573 The CDF values using Ti as an invariant element (**Table 4**) showed important discrepancies
574 (i.e., values from 2 to -1670%) between different soil samples, including even the samples
575 taken within the same soil profile (K-8 and V-9 soil samples). These differences are not
576 linked to the nature of parental rock (i.e., mafic vs felsic). Positive CDF values in samples K-
577 7, K-14 and K-37 can be related to chemical losses from the parental material whereas

578 negative values in K-29, V-4, V-7 and V-16 can be attributed to fresh mineral supply to the
579 regolith. In soils where chemical dedudation seems to occur, positive CDF values should
580 decrease or remain constant from surface to depth. This was only observed in K-7 and K-37
581 soils. Thus, even for soil with positive CDF, the pathway and rate of chemical weathering
582 cannot be constrained. When chemical depletion fraction of individual element is considered
583 (**Table 4**), only K-14 B₁ and C horizons samples show positive values for all considered
584 element. Chemical depletion fraction of individual element confirm the relative enrichment of
585 soil samples in K and to a lesser extend in Na compared to the parental rocks. Some samples,
586 however, dis not exhibit relative enrichment in K (K-29 samples, V-9 A and V-15 O/A
587 horizon samples) or in Na (K-8 E, K-37 O, K-37 A, V-9 O, V-9 A and V-15 O/A horizon
588 samples) suggesting diverse origin of chemical supply to the soils. For example, K-29 soil
589 samples developed over felsic formation (i.e., granite/gneiss) showed negative CDF values in
590 Na, Ca, Al and Si. The enrichments in Si and Al are difficult to interpret as they mainly occur
591 in horizons presenting spodic properties that can result from element mobilisation within the
592 soil profile.

593 Another widely used proxy for chemical weathering intensity of source rocks for soils
594 and sediments is Chemical Index of Alteration (CIA; Nesbitt and Young, 1982; Fedo et al.,
595 1995, Li and Yang, 2010). It is calculated using the molar proportion of major elements, as
596 follows:

$$597 \quad \text{CIA} = [\text{Al}_2\text{O}_3 / (\text{Al}_2\text{O}_3 + \text{CaO}^* + \text{Na}_2\text{O} + \text{K}_2\text{O})] \times 100$$

598 where CaO* used in the CIA calculation refers to CaO from the silicate fraction exclusively.
599 Basic rocks exhibit average CIA values (42 and 36 for Kivakka layered intrusion and Vetreny
600 Belt paleorift respectively) which are lower than the CIA of felsic rocks (CIA value of
601 archean granite ~50). It can be observed that the CIA of soils is not always higher than that of
602 their respective parent rocks (**Table 4**). The ratio $\text{CIA}_{\text{soil sample}} / \text{CIA}_{\text{parent rock}}$ is considered as a

603 proxy of the “weathering degree” of a soil. Some samples (V-15, V-9, K-8-C, all the K-29
604 samples) show CIA_s/CIA_r values lower than 1. Since the CIA calculation involves Al (thought
605 to be rather mobile during podzolisation) and K (a nutrient highly recycled by vegetation),
606 several hypotheses can explain this CIA value: 1) the loss of Al during weathering of K-
607 feldspars and downward migration due to podzolisation occurring mainly in E horizon; 2) the
608 accumulation of K from buried organic matter in the form of plant litter in the uppermost
609 organic-rich soil horizons, and 3) the input of K, Al, Ca, and Na from allochthonous sources.

610 Al loss during podzolisation usually affects the O, A and E horizons (Melkerud et al.,
611 2000; Olsson et al., 2000; Giesler et al., 2000); K incorporation may affect O horizon and the
612 effect of addition of allochthonous material depends on its origin (e. g. aeolian, morainic) and
613 composition. Incorporation of allochthonous material may actually lead to a “dilution” effect
614 thus underestimating the element content in the soil profile. As a result, even at zero level of
615 chemical weathering intensity, the presence of moraine or aeolian material can lead to an
616 under- or overestimation of the CIA depending on the chemical composition of the mineral
617 supply. Except in a few samples mentioned above, most soils developed on mafic rocks
618 showed $CIA_s/CIA_r > 1$ which is higher than that in soils over felsic formation ($CIA_s/CIA_r \sim 1$).
619 However, the dilution effect of the moraine was more pronounced for basic rocks compared to
620 acidic rocks because of the felsic dominant nature of the moraine.

621 Mineralogical studies performed on soils samples show the presence of ubiquitous
622 quartz (and in some soils, zircon) independent on the nature of the parental rocks. The size of
623 quartz grains varied from 10 to 450 μm and from 50 to 200 μm in soils developed on mafic
624 and felsic rocks, respectively, which precluded an aeolian origin of these quartz grains. In
625 contrast, quaternary (Pleistocene) deposits observed even in the deepest horizons of some soil
626 profiles (**Fig. 4 E**) confirm a strong moraine influence in this region. This moraine altered
627 significantly the chemistry of soils as it can be seen on the WIS diagram (**Fig. 5, Table 4**) that

628 take into account a silica component (Meunier et al., 2013). All studied rocks fall in their
629 respective “domain” within the WIS diagram. On the opposite, soils samples, whatever their
630 parental rock, fall in the “felsic domain”, with the exception of the V-7 C, K-14, V-15 and V-
631 9 soils samples. Only the K-14 B1 and K-14 C samples are plotted close to the parental
632 olivenite suggesting a poor influence of allochthonous morainic material in K-14 soil
633 pedogenesis. In the felsic domain, TTG and glacial till (Lunkka et al., 2013) are chemically
634 similar with silica content lower than soils samples. This is coherent with chemical
635 weathering processes in cold environment wich involve relative enrichment in silica (quartz
636 preservation) in comparison with the alkaline earth elements (M^+ pole; $Na^+ + K^+ + 2Ca^{2+}$) or
637 the divalent metallic elements (R^{2+} pole; $Mg^{2+} + Fe^{2+} + Mn^{2+}$) that are lost from the soil
638 during pedogenesis. This trend is particularly pronounced when comparing E and B horizons
639 of podzolic soils on the WIS diagram. E horizons are systematically closer to the 4Si pole
640 than the B horizon. Such results suggest that, even if a strong morainic influence has
641 completely modified the mineralogical and chemical nature of the initial regolith, the soil
642 forming processes such as podzolisation occurring within these soils are similar and
643 consistent among different sites.

644

645 5.1.2. REE fractionation between rocks and soils

646 Five horizons of a soil developed on gabbro-norites (sample K-37 from the Kivakka
647 intrusion, **Fig. 6 A**) show enrichment in light rare earth elements (LREE) and depletion in
648 heavy rare earth elements (HREE) relative to the gabbro-norite. Enrichment in LREE was
649 also observed by Öhlander et al. (1996) in B-horizons of spodosols developed on felsic till in
650 northern Sweden, whereas E-horizons were depleted in all REE, with LREE being more
651 depleted than HREE. According to Öhlander et al. (1996), this secondary enrichment in B-
652 horizons could be caused by adsorption on secondary oxy-hydroxides, on clay minerals or

653 organic material, or by the precipitation of secondary LREE enriched phosphates. Note the
654 higher affinity of LREE to adsorb on oxy(hydr)oxides and the tendency of HREE to form
655 more stable dissolved complexes than LREE in solution (Bau, 1999) is in agreement with
656 these tendencies.

657 Olivinite rock is enriched in HREE, and sample K-14 B₂ from the Kivakka intrusion
658 (**Fig. 6 B**) is enriched in all REE relative to olivinite for all horizons of the soil profile. On the
659 contrary, soils developed on felsic rocks (samples K-7, K-8, K-29 from Kivakka intrusion,
660 **Fig. 6 C**) have inverted REE concentrations with respect to parental granite, all horizons are
661 depleted in REE relative to the source rock. The REE patterns of soils developed both on
662 mafic and felsic rocks in the Vetreny Belt zone (**Fig. 6 D**) demonstrate that soils developed
663 on basalt (samples V-4 and V-7) are depleted in REE with respect to parental rock with the
664 exception of the B horizon of V-7 which is slightly enriched in LREE. Soils over felsic rock
665 are also more significantly depleted in all REE relative to the source TTG. However, it can be
666 seen that patterns of soils with different origins (mafic or felsic) are quite similar. This is
667 further illustrated in **Fig. 6 E** where the E or B horizons of different soils developed on both
668 felsic (K-7, K-8, K-29) and mafic (K-14, K-37) rocks are plotted. It demonstrates that the
669 REE fractionation in intermediate horizons in all studied soils is identical regardless of the
670 underlying rock. This result is in agreement with observations of Lesovaya et al. (2008) on
671 podzols and podzolized podburs on mafic substrates under the influence of glacial moraine
672 deposits in mountainous taiga areas in northwestern Russia. According to these authors, the
673 mineralogical effect of the admixture of gneiss-derived material is, in general, most
674 pronounced in the E horizon.

675

676

677

678 *5.2. Actual weathering processes: waters versus soils and rocks*

679 A binary logarithmic diagram of the molar Ca/Na versus Mg/Na ratios in rocks, soils
680 and waters, including atmospheric precipitation shows that the Ca/Na ratio ranges from 0.2 to
681 8.6 and 0.25 to 5.8 for soils and waters, respectively (**Fig. 9**). The Mg/Na ratio varies between
682 0.15 and 8.9 for waters, and between 0.1 and 1.9 for soils; the highest ratio of 76.5 and 214.3
683 are for soil K-14 on olivinite (B₁ and C horizons, respectively). There is a good correlation
684 between Ca/Na and Mg/Na ratios in soils and rocks, and between surface waters and rocks.
685 The majority of samples from the Kivakka intrusion and the Vetreny Belt, exempting soils K-
686 29 (horizon E) and K-14 (horizons B₁ and C) which drop out of the tendency, are located on
687 the mixing line between silicate and carbonate end-members although no clear evidence of
688 carbonate phases was previously described for neither rocks nor soils and no carbonate
689 mineral was found within the resolution of XRD analysis of soils.

690 Lower Ca/Na and Mg/Na ratio for soils compared to rocks is consistent with on-going
691 chemical weathering, as calcium-rich phases usually weather more rapidly than sodium-rich
692 phases in silicate environments. In this regard, the addition of moraine material enriched in
693 Na (Na-K feldspar) can also explain this tendency. Lesovaya et al. (2008) observed the
694 presence of moraine admixtures in mafic rock-soil systems, expressed in the lower content of
695 calcium in the middle taiga soils of Karelia which could be due to the admixture of stable K-
696 Na feldspars.

697 Stream waters are known to have higher Ca/Na molar ratio than rocks and soils and
698 should exhibit lower Ca/Na ratio compared to parental rocks (Gaillardet et al., 1999; Oliva et
699 al., 2004). We observe different tendencies of water composition: surface waters are situated
700 either in the same region or are enriched in Ca or Mg compared to soils in the case of the
701 Vetreny Belt rock-soil-water system. For the Kivakka intrusion system the surface fluids are
702 located between the soil and rock reservoirs reflecting preferential mobilisation of sodium

703 relative to calcium or magnesium in these surface waters as compared to rocks. The waters
704 from the Vetreny Belt mafic rocks exhibit higher Mg/Na and lower Ca/Na ratios compared to
705 the Kivakka basic massif and surrounding felsic rocks, which is in agreement with higher Mg
706 concentrations in basalts of the Vetreny Belt (up to 20-25 % MgO in spinifex-like structures,
707 see Kulikov et al., 2005).

708 Unexpectedly, surface waters draining felsic environments show higher Ca/Na and
709 Mg/Na molar ratios than waters draining mafic rocks. This relative enrichment in Na with
710 respect to Ca and Mg in rivers from mafic watersheds compared to felsic watershed may be
711 explained by a higher mobility of sodium compared to Ca and Mg during the weathering
712 process and the retention of Mg and Ca during secondary phases forming. It is possible that
713 Ca and Mg, unlike Na, participate in secondary mineral formation such as Mg-vermiculite.
714 Some Ca and Mg rich phases (i. e. CaMg-amphibole) can also weather less rapidly than Na-
715 rich feldspar (Salminen et al., 2008). Soil K-14 which is over olivinite (B and C horizons)
716 exhibited a clear tendency of enrichment in Mg and Ca compared to Na during basic rock
717 weathering. This is consistent with the presence of Mg-vermiculite and CaMg-amphibole in
718 the clay fraction. The persistence of Ca-amphibole in such soils has been also observed by
719 Lesovaya et al. (2008).

720 Consistent with these chemical and mineralogical observations, the radiogenic
721 isotopes demonstrate two features of the water-soil-rock system development in NW Russia
722 (**Fig. 8**): (1) During different stages of weathering, easily weatherable and less radiogenic
723 minerals (secondary clays, carbonates) were strongly consumed throughout the full depth of
724 examined soil profile. This provided a more radiogenic Sr isotopic signature to most soils
725 developed on mafic rocks compared to that of the parent rocks which was especially
726 pronounced in the surface horizons. For both the Kivakka intrusion and the Vetreny Belt, we
727 observe a shift of $^{87}\text{Sr}/^{86}\text{Sr}$ from ~ 0.705 (rocks) to 0.715-0.725 (soils). The same behaviour

728 was reported for soils developed over basalts in Central Siberia (Bagard et al., 2013). Second,
729 all the granitic moraine in Karelian region had a more radiogenic signature than the studied
730 bedrocks. Isotope signatures of waters draining through both felsic and mafic zone reflect the
731 weathering of more radiogenic minerals. However, these radiogenic signatures are lower than
732 that reported by Land et al. (2000) for stream waters (~0.74) draining felsic rocks in northern
733 Sweden within the Kalix river watershed.

734

735 *5.3. Chemical weathering rates*

736 In general, the composition of surface waters does not reflect a purely felsic or mafic
737 source being similar in all waters, except for one Mg-rich surface water draining through
738 olivinite environment of the Kivakka intrusion (sample K-13-w). The surface waters draining
739 through both Kivakka and Vetreny Belt region are strongly oversaturated with respect to
740 $\text{Al}(\text{OH})_3$, boehmite, gibbsite, halloysite, imogolite, kaolinite, ferrihydrite (factor 10 to 10^6),
741 and undersaturated with respect to amorphous silica, and close to saturation with quartz.
742 Apparently, the amorphous, organic-rich Al and Fe oxyhydroxides and silicates constitute a
743 major part of secondary phases in soils as is well known for boreal zone (Lundström et al.,
744 2000, Giesler et al., 2000). One particular feature in soil K-14 is the occurrence of Mg-
745 vermiculite and a high pH. Processes usually occurring in podzolic soils are rock dismantling,
746 Al- and Fe-organic complex formation, organic matter modification, oxidation of iron bearing
747 primary phases, and amorphous alumino-silicate precipitation. However, the podzolation
748 process is known to rarely produce any clay mineral formation and clays are relatively absent
749 (Mokma et al., 2004).

750 Only the K-14-C soil sample was not affected by moraine deposit, and thus, it can be
751 used in calculation of weathering rates of basic rocks. Our results give a long term TDS
752 weathering rate of 1184 eq/ha/yr for olivinite rock, which is 4 times higher than the long term

753 base cation flux (360 eq/ha/yr) and about 2 times higher than the actual TDS weathering rate
754 (~700 eq/ha/yr) estimated by Land et al. (1999) for granitic till in northern Sweden. This
755 value corresponds to a long term weathering rate of ~1.5 t/km²/yr which is lower than the
756 present day weathering rate estimated by Zakharova et al. (2007) and Pokrovsky et al. (2005)
757 for Karelian and Siberian mafic rocks (2.3 and 5-6 t/km²/y, respectively) but comparable with
758 chemical denudation rates of Canadian granites (0.35 to 1.55 t/km²/y for Slave Province vs
759 Grenville, Millot et al., 2002). Calculation of weathering fluxes were conducted for A and B₁
760 horizons and give values of 364 eq/ha/yr and 148 eq/ha/yr, respectively, which are consistent
761 with fluxes reported by Land et al. (1999) for the granitic till, and for podzol soils covered by
762 Norway spruce in Sweden (344 eq/ha/yr for Ca+Mg+Na+K, Simonsson et al., 2015). These
763 values are sizebly lower than the base cations release rate, calculated for similar
764 environmental context using various mineral dissolution models (1400-2700 eq/ha/yr,
765 Erlandsson et al., 2016).

766 Results of the present study demonstrate that the weathering rates of ultramafic rocks
767 are higher than those of the felsic till, but dominant moraine deposits in this region hide the
768 true magnitude of weathering processes. The dominant mechanism responsible for slowing
769 the rates of mafic rock weathering could be retention of Mg and Ca in soil are likely due to
770 precipitation of secondary phases such as Mg-vermiculite or adsorption on mineral, organic,
771 or organo-mineral phases.

772

773 **6. Conclusions**

774 A multidisciplinary study of mafic rocks weathering in the region affected by glacial
775 moraine deposits (northwestern Russia) demonstrated the following:

776 (1) Traces of chemical corrosion on the surface of zircons and feldspars along with the
777 presence of new-formed amorphous matter on the surface of quartz, plagioclases and

778 pyroxenes are evidence of similar weathering processes on all types of parental rock.
779 However, the lack of kaolinite neoformation and the persistence of amphibole and plagioclase
780 feldspar in soils suggest not very intense weathering processes, in accordance with a start of
781 pedogenesis about 10 Ky ago.

782 (2) The presence of quartz and zircon in soils developed on basic rocks, similarity of
783 REE patterns of intermediate and deep soil horizons both for felsic and mafic rocks, and the
784 isotopic signature of soils on gabbro-norite and olivinite similar to that of granodiorites raise a
785 question of the polycyclic nature of these soils (soil developed on fragments of already pre-
786 existing soil), and assume their “contamination” with exterior deposits such as granitic
787 moraine.

788 (3) The relative enrichment in Na with respect to Ca and Mg in rivers from both felsic
789 and mafic watersheds suggests a contribution from other sources than primary silicate
790 weathering reactions. We suggest that either Mg-vermiculite and Ca, Mg-amphibole
791 formation in soils limits Ca and Mg release to surface waters, or that there are highly
792 weatherable Ca- and Mg-rich minerals present in felsic rocks. These specific features should
793 be taken into account in estimation of mafic rocks weathering rates and calculations of
794 atmospheric CO₂ consumption for weathering in such a particular environment.

795 (4) The radiogenic isotopes of the water-soil-rock system development in NW Russia
796 demonstrated *i*) preferential removal of easily weatherable and less radiogenic minerals
797 throughout the full depth of soil profile, and *ii*) more radiogenic signature of the granitic
798 moraine compared to mafic and felsic bedrocks.

799 (5) In the cold subarctic climate, even thin deposits of glacial till moraine are capable
800 of “protecting” mafic rocks from direct chemical weathering. As a result, over 10 000-
801 15 000 years of exposure after the last glaciation, full weathering soil profiles on basic rocks
802 could not be established.

803 (6) The weathering rates of ultramafic rocks are higher than those from felsic till, but
804 widespread moraine depositions in this region hide the magnitude of weathering processes.
805 These findings may have broad applications for reconstructing paleo environments and
806 quantifying the true capacity of igneous silicate rocks to absorb CO₂ during weathering in
807 high latitude regions.

808

809 **Acknowledgements**

810 Authors are grateful to F. Candaudap, Th. Aigouy, Ph. and F. de Parceval, and P. Brunet for
811 analytical support. C. Benker is thanked for thorough English proofread. Partial support from
812 the TSU competitiveness improvement programme Project N 8.1.04.2018 is acknowledged.

813

814 **References**

- 815 AFNOR, 1996. Qualité des sols. Recueil de normes Françaises, Association Française de
816 Normalisation, Paris.
- 817 Akselsson, C., Holmqvist, J., Kurz, D., Sverdrup, H., 2006. Relations between elemental
818 content in till, mineralogy of till and bedrock mineralogy in the province of Småland,
819 southern Sweden. *Geoderma* 136, 643-659.
- 820 Alapieti, T., 1982. The Koillismaa layered igneous complex, Finland: its structure,
821 mineralogy and geochemistry, with emphasis on the distribution of chromium. *Bull.*
822 *Geol. Surv. Finl.* 319, 116.
- 823 Allen, C., Darmody, R., Thorn, C., Dixon, J., Schlyter, P., 2001. Clay mineralogy, chemical
824 weathering and landscape evolution in Arctic-Alpine Sweden. *Geoderma* 99, 277-294.
- 825 Amelin, Y., Semenov, V., 1990. On the age and sources of magmas for the early Proterozoic
826 layered intrusions of Karelia (abstracts of contributions). *Isotopic dating of endogenic*
827 *ore associations, Tbilisi*, 40-42.
- 828 Amelin, Y.V., Semenov, V.S., 1990. Age and magma source of the early Paleoproterozoic
829 layered intrusions of Karelia (in Russian). In *Proceedings of all-USSR conference*
830 *“Isotope dating of endogenous ore formations”*, XXIV session, Tbilisi, November 12-
831 18, 1990, 40-42. Amelin, Y.V., Heaman, L., Semenov, V., 1995. U-Pb geochronology
832 of layered mafic intrusions in the eastern Baltic Shield: implications for the timing and
833 duration of Paleoproterozoic continental rifting. *Precambrian Res.* 75, 31-46.
- 834 Amelin, Y.V., Semenov, V.S., 1996. Nd and Sr isotopic geochemistry of mafic layered
835 intrusions in the eastern Baltic shield: implications for the evolution of
836 Paleoproterozoic continental mafic magmas. *Contrib. Mineral. Petrol.* 124, 255-272.
- 837 Ameijeiras-Marino, Y., Opfergelt, S., Schoonejans, J., Vanacker, V., Sonnet, P., de Jong, J.,
838 Delmelle, P., 2017. Impact of low denudation rates on soil chemical weathering
839 intensity: A multiproxy approach. *Chem. Geol.* 456, 72-84.
- 840 Anderson, H., Berrow, M., Farmer, V., Hepburn, A., Russell, J., Walker, A., 1982. A
841 reassessment of podzol formation processes. *J. Soil Sci.* 33, 125-136.
- 842 Andersson, P. S., Porcelli, D., Gustafsson, O., Ingri, J., Wasserburg, G. J., 2001. The
843 importance of colloids for the behavior of uranium isotopes in the low-salinity zone of

- 844 a stable estuary. *Geochim. Cosmochim. Acta* 65(1), 13–25.
- 845 Andersson, K., Dahlqvist, R., Turner, D., Stolpe, B., Larsson, T., Ingri, J., Andersson, P.,
846 2006. Colloidal rare earth elements in a boreal river: Changing sources and
847 distributions during the spring flood. *Geochim. Cosmochim. Acta* 70, 3261-3274.
- 848 Andrews, L.C., Catania, G.A., Hoffman, M.J., Gulley, J.D., Lüthi, M.P., Ryser, C., Hawley,
849 R.L., Neumann, T.A., 2014. Direct observations of evolving subglacial drainage
850 beneath the Greenland Ice Sheet. *Nature* 514, 80-83.
- 851 Bagard M.-L., Schmitt A.-D., Chabaux F., Pokrovsky O.S., Viers J., Stille P., Labolle F.,
852 Prokushkin A.S. (2013) Biogeochemistry of stable Ca and radiogenic Sr isotopes in
853 larch-covered permafrost-dominated watersheds of Central Siberia. *Geochimica*
854 *Cosmochimica Acta*, 114, 169–187.
- 855 Balagizi, C., Darchambeau, F., Bouillon, S., Yalire, M., Lambert, T., Borges, A., 2015. River
856 geochemistry, chemical weathering, and atmospheric CO₂ consumption rates in the
857 Virunga Volcanic Province (East Africa). *G³*, 16, 2637-2660.
- 858 Balashov, Y.A., Bayanova, T.B., Mitrofanov, F. P., 1993. Isotope data on the age and genesis
859 of layered basic-ultrabasic intrusions in the Kola Peninsula and northern Karelia,
860 northeastern Baltic Shield. *Precambrian Res.* 64, 197-205.
- 861 Barkov, A., Gannibal, L., Ryungenen, G., Balashov, Y., 1991. Zircon dating of the Kivakka
862 layers massif, Northern Karelia. Abstracts of papers. All-USSR seminar on methods
863 of isotopic geology, Zvenigorod, 21-25 October 1991, St. Petersburg, 21-23.
- 864 Bau, M., 1999. Scavenging of dissolved yttrium and rare earths by precipitating iron
865 oxyhydroxide: Experimental evidence for Ce oxidation, Y-Ho fractionation, and
866 lanthanide tetrad effect. *Geochim. Cosmochim. Acta* 63, 67-77.
- 867 Berner, R. A., Lasaga, A. C., Garrels, R. M., 1983. The carbonate-silicate geochemical cycle
868 and its effect on atmospheric carbon dioxide over the past 100 million years. *Am. J.*
869 *Sci.* 283, 641-683.
- 870 Berner, R., 1992. Weathering, plants, and the long-term carbon cycle. *Geochim. Cosmochim.*
871 *Acta* 56(8), 3225-3231.
- 872 Berner, R., 1995. Chemical weathering and its effect on atmospheric CO₂ and climate.
873 *Reviews in Mineralogy and Geochemistry* 31(1), 565-583.
- 874 Berner, R., Caldeira, K., 1997. The need for mass balance and feedback in the geochemical
875 carbon cycle. *Geology* 25, 955-956. Bibikova, E. V., Samsonov, A. V., Petrova, A. Y.,
876 Kirnozova, T. I., 2005. The Archean geochronology of Western Karelia. *Stratigraphy*
877 *and Geological Correlation* 13(5), 459-475.
- 878 Boeglin, J., Probst, J., 1998. Physical and chemical weathering rates and CO₂ consumption in
879 a tropical lateritic environment: the upper Niger basin. *Chem. Geol.* 148(3-4), 137-
880 156.
- 881 Brady, P.V., 1991. The Effect of silicate weathering on global temperature and atmospheric
882 CO₂. *Journal of Geophysical Research* 96(B11), 18101-18106.
- 883 Breemen van, N., Buurman, P., 1998. *Soil Formation*, 245-270. Kluwer Academic Publishers,
884 Dordrecht, Boston.
- 885 Brimhall, G. H., Lewis, C. J., Ford, C., Bratt, J., Taylor, G., Warin, O., 1991. Quantitative
886 geochemical approach to pedogenesis: importance of parent material reduction,
887 volumetric expansion, and eolian influx in lateritization. *Geoderma* 51, 51-91.
- 888 Buurman, P., 1984. *Podzols: Temperate regions* (Van Nostand Reinhold soil science series).
889 Van Nostand Reinhold, New York. Buurman, P., Jongmans, A., 2005. Podzolisation
890 and soil organic matter dynamics. *Geoderma* 125(1-2), 71-83.
- 891 Bychkova, Y.V., 2003. Structural patterns of contrasting rhythmic layering of Kivakka
892 intrusion. PhD thesis, Moscow State University.
- 893 Bychkova, Y., Koptev-Dvornikov, E., 2004. Rhythmical layering of Kivakka type: geology,

- 894 petrology, petrochemistry, hypothesis of formation (in Russian). *Petrology* 12(3), 281-
895 302.
- 896 Bychkova, Y. V., Koptev-Dvornikov, E. V., Kononkova, N. N., Kameneva, E. E., 2007.
897 Composition of rock-forming minerals in the Kivakka layered massif, Northern
898 Karelia, and systematic variations in the chemistries of minerals in the rhythmic
899 layering subzone. *Geochemistry International* 45(2), 131–151.
- 900 Caritat de, P., Reimann, C., Bogatyrev, I., Chekushin, V., Finne, T. E., Halleraker, J. H.,
901 Kashulina, G., Niskavaara, H., Pavlov, V., Ayras, M., 2001. Regional distribution of
902 Al, B, Ba, Ca, K, La, Mg, Mn, Na, P, Rb, Si, Sr, Th, U and Y in terrestrial moss within
903 a 188,000 km² area of the central Barents region: influence of geology, seaspray and
904 human activity. *Appl. Geochem.* 16, 137-159.
- 905 Condie, K. C., 1993. Chemical composition and evolution of the upper continental crust:
906 Contrasting results from surface samples and shales. *Chem. Geol.* 104(1-4), 1-37.
- 907 Cornu, S., Lucas, Y., Lebon, E., Ambrosi, J. P., Luizão, F., Rouiller, J., Bonnay, M., Neal, C.,
908 1999. Evidence of titanium mobility in soil profiles, Manaus, central Amazonia.
909 *Geoderma* 91(3-4), 281-295.
- 910 Courchesne, F., Hendershot, W., 1997. Essai. La Genèse des podzols', *Geogr. Phys. Quarter.*
911 51, 235-250.
- 912 Dahlqvist, R., Benedetti, M. F., Andersson, K., Turner, D., Larsson, T., Stolpe, B., Ingri, J.,
913 2004. Association of calcium with colloidal particles and speciation of calcium in the
914 Kalix and Amazon rivers. *Geochim. Cosmochim. Acta* 68(20), 4059-4075.
- 915 Dahlqvist, R., Andersson, K., Ingri, J., Larsson, T., Stolpe, B., Turner, D., 2007. Temporal
916 variations of colloidal carrier phases and associated trace elements in a boreal river.
917 *Geochim. Cosmochim. Acta* 71, 5339-5354.
- 918 D'Amico, M., Julitta, F., Previtali, F., Cantelli, D., 2008. Podzolization over ophiolitic
919 materials in the western Alps (Natural Park of Mont Avic, Aosta Valley, Italy).
920 *Geoderma* 146, 129-137.
- 921 Debon, F., Enrique, P., Autran, A., 1995. Magmatisme Hercynien. Synthèse géologique et
922 géophysique des Pyrenees. Edt BRGM 1, Cycle Hercynien (eds. A. Barnolas and J. C.
923 Chiron), 361-499.
- 924 DePaolo, D., Wasserburg, G., 1976. Inferences about magma sources and mantle structure
925 from variations of ¹⁴³Nd/¹⁴⁴Nd. *Geophys. Res. Lett.* 3, 249-252.
- 926 DePaolo, D. J., 1981. Neodymium isotopes in the Colorado Front Range and crust-mantle
927 evolution in the Proterozoic. *Nature* 291, 193-196.
- 928 DePaolo, D., 1988. Neodymium isotope geochemistry: an introduction. Springer-Verlag, New
929 York, p. 187.
- 930 Dessert, C., Dupré, B., Francois, L. M., Schott, J., Gaillardet, J., Chakrapani, G., Bajpai, S.,
931 2001. Erosion of Deccan Traps determined by river geochemistry: impact on the
932 global climate and the ⁸⁷Sr/⁸⁶Sr ratio of seawater. *Earth Planet. Sci. Lett.* 188, 459-474.
- 933 Dessert, C., Dupré, B., Gaillardet, J., François, L. M., Allègre, C. J., 2003. Basalt weathering
934 laws and the impact of basalt weathering on the global carbon cycle. *Chem. Geol.* 202,
935 257-273.
- 936 Dessert, C., Lajeunesse, E., Lloret, E., Clergue, C., Crispi, O., Gorge, C., Quidelleur, X.,
937 2015. Controls on chemical weathering on a mountainous volcanic tropical island:
938 Guadeloupe (French West Indies). *Geochimica et Cosmochimica Acta* 171, Pages
939 216-237. Deuerling, K.M., Martin, J.B., Martin, E.E., Scribner, C.A., 2018. Hydrologic
940 exchange and chemical weathering in a proglacial watershed near Kangerlussuaq, west
941 Greenland. *J. Hydrol.* 556, 220-232.
- 942 Dokuchaev, V., 1880. On podzol (in Russian). *Trudy Volnogo ekonomicheskogo obschestva*
943 1(2), 142-150.

- 944 Dupré, B., Gaillardet, J., Rousseau, D., Allègre, C. J., 1996. Major and trace elements of
 945 river-borne material: The Congo Basin. *Geochim. Cosmochim. Acta* 60(8), 1301-
 946 1321.
- 947 Dupré, B., Dessert, C., Oliva, P., Godderis, Y., Viers, J., Francois, L., Millot, R., Gaillardet,
 948 J., 2003. Rivers, chemical weathering and Earth's climate. *C. R. Geoscience* 335,
 949 1141-1160.
- 950 Eiriksdottir, E., Gislason, S., and Oelkers, E., 2013. Does temperature or runoff control the
 951 feedback between chemical denudation and climate? Insights from NE Iceland:
 952 *Geochimica et Cosmochimica Acta*, v. 107, p. 65–81
- 953 Eiriksdottir, E.S., Gislason, S.R., Oelkers, E.H., 2015. Direct evidence of the feedback
 954 between climate and nutrient, major, and trace element transport to the oceans.
 955 *Geochim. Cosmochim. Acta* 166, 249-266.
- 956 Erlandsson, M., Oelkers, E.H., Bishop, K., Sverdrup, H., Belyazid, S., Ledesma, J.L.J.,
 957 Köhler, S.J., 2016. Spatial and temporal variations of base cation release from
 958 chemical weathering on a hillslope scale. *Chemical Geol.* 441, 1-13.
- 959 Fedo, C. M., Nesbitt, H. W., Young, G. M., 1995. Unraveling the effects of potassium
 960 metasomatism in sedimentary rocks and paleosols, with implications for
 961 paleoweathering conditions and provenance. *Geology* 23(10), 921-924.
- 962 Feoktistov, V. M., 2004. Water chemical composition of Karelian rivers and their dissolved
 963 chemical discharge into the White Sea. *Water Resour.* 31(6), 631-638.
- 964 Ferrier, K. L., Riebe, C. S., Hahm, W. J., 2016. Testing for supply-limited and kinetic-limited
 965 chemical erosion in field measurements of regolith production and chemical depletion,
 966 *Geochem. Geophys. Geosyst.* 17, 2270–2285.
- 967 Foster, G.L., Vance, D., 2006. Negligible glacial-interglacial variation in continental chemical
 968 weathering rates. *Nature* 444, 918-921.
- 969 Gaillardet, J., Dupré, B., Louvat, P., Allègre, C., 1999. Global silicate weathering and CO₂
 970 consumption rates deduced from the chemistry of large rivers. *Chem. Geol.* 159, 3-30.
- 971 Gaillardet, J., Rad, S., Rive, K., Louvat, P., Gorge, C., Allègre, C.J., Lajeunesse, E., 2011.
 972 Orography-driven chemical denudation in the Lesser Antilles: Evidence for a new
 973 feed-back mechanism stabilizing atmospheric CO₂. *American Journal of Science* 311,
 974 851-894.
- 975 Giesler, R., Ilvesniemi, H., Nyberg, L., van Hees, P., Starr, M., Bishop, K.,
 976 Kareinen, T., Lundström, U., 2000. Distribution and mobilization of Al, Fe and Si in
 977 three podzolic soil profiles in relation to the humus layer. *Geoderma* 94, 249-263.
- 978 Gislason, S. R., Arnorsson, S., Armannsson, H., 1996. Chemical weathering of basalt in
 979 Southwest Iceland, effects of runoff, age of rocks and vegetative/glacial cover.
 980 *American Journal of Science* 296, 837-907.
- 981 Goldstein, S., O'Nions, R., Hamilton, P. 1984. A Sm-Nd study of atmospheric dusts and
 982 particulates from major river system. *Earth Planet. Sci. Lett.* 70, 221-236.
- 983 Grard, A., François, L., Dessert, C., Dupré, B., Goddérís, Y., 2005. Basaltic volcanism and
 984 mass extinction at the Permo-Triassic boundary: Environmental impact and modeling
 985 of the global carbon cycle. *Earth Planet. Sci. Lett.* 234(1-2), 207-221.
- 986 Hättestrand, C. (1997), Ribbed moraines in Sweden – distribution pattern and
 987 palaeoglaciological implications, *Sedimentary Geology* 111, 41-56.
- 988 Hawley, S.M., Pogge von Strandmann, P.A.E., Burton, K.W., Williams, H.M., Gislason, S.R.,
 989 2017. Continental weathering and terrestrial (oxyhydr)oxide export: Comparing glacial
 990 and non-glacial catchments in Iceland. *Chem. Geol.* 462, 55-66.
- 991 Hindshaw, R.S., Rickli, J.R., Leuthold, J., Wadham, J., Bourdon, B., 2014. Identifying
 992 weathering sources and processes in an outlet glacier of the Greenland Ice Sheet using
 993 Ca and Sr isotope ratios. *Geochim. Cosmochim. Acta* 145, 50-71.
- 994 Horton, T., Chamberlain, C.P., Fantle, M., Blum, J., 1999. Chemical weathering and

- 994 lithologic controls of water chemistry in a high-elevation river system: Clark's Fork of
 995 the Yellowstone river, Wyoming and Montana. *Water Resour. Res.*, 35, 1643-1655.
- 996 Ibarra, D., Caves, J., Moon, S., Thomas, D., Hartmann, J., Page Chamberlain, C., Maher, K.,
 997 2016. Differential weathering of basaltic and granitic catchments from concentration-
 998 discharge relationships. *Geochimica et Cosmochimica Acta* 190, 265-293.
- 999 Ingri, J., Widerlund, A., Land, M., Gustafsson, O., Andersson, P. S., Öhlander, B., 2000.
 1000 Temporal variations in the fractionation of the rare earth elements in a boreal river, the
 1001 role of colloidal particles. *Chem. Geol.* 166, 23-45.
- 1002 Ingri, J., Widerlund, A., Land, M., 2005. Geochemistry of major elements in a pristine boreal
 1003 river system, hydrological compartments and flow paths. *Aquatic Geochemistry* 11,
 1004 57-88.
- 1005 Jacobsen, S. B., Wasserburg, G., 1980. Sm-Nd isotopic evolution of chondrites. *Earth Planet.*
 1006 *Sci. Lett.* 50(1), 139-155.
- 1007 Kempton, P. D., Downes, H., Neymark, L. A., Wartho, J. A., Zartman, R. E., Sharkov, E. V.,
 1008 2001. Garnet granulite xenoliths from the northern Baltic Shield – the underplated
 1009 lower crust of a palaeoproterozoic large igneous province? *J. Petrol.* 42(4), 731-763.
- 1010 Klyunin, S., Grokhovskaya, T., Zakharov, A., Solovjeva, T., 1994. Geology and platinum-
 1011 bearing potential of the Olanga group of massifs, Northern Karelia (in Russian).
 1012 *Geologiya i genesis mestorozhdenii platinovykh metallov.* Nauka, Moscow, 111-126.
- 1013 Koptev-Dvornikov, E. V., 2001. Distribution of cumulative mineral assemblages, major and
 1014 trace elements over the vertical c of the Kivakka intrusion, Olanga group of intrusions,
 1015 Northern Karelia. *Petrology* 9(1), 3-27.
- 1016 Kulikov, V., Kulikova, V., 1982. On the summary section of the early Precambrian of the
 1017 Vetreny belt (in Russian). *Geology and Stratigraphy of Karelian Precambrian Rocks.*
 1018 *Petrozavodsk, Year Book Information*, 21-26.
- 1019 Kulikov, V., 1999. Komatiitic Basalts of the Vetreny Belt (in Russian). *Selected Works of the*
 1020 *Karelian Scientific Center of Russian Academy of Sciences*, 60-61.
- 1021 Kulikov, V., Kulikova, V., Bychkova, Y., Zudin, A., 2003. Sumian rifting volcanism of
 1022 Paleoproterozoi in South-Eastern part of Karelian Kraton. *Proceedings of the II All-*
 1023 *Russian symposium on volcanology and paleovolcanology "Vulkanizm i*
 1024 *geodinamika". Ekaterinburg*, 99-104.
- 1025 Kulikov, V., Bychkova, Y., Kulikova, V., Koptev-Dvornikov, E., Zudin, A., 2005. Role of
 1026 deep-seated differentiation in formation of Paleoproterozoic Sinegorie lava plateau of
 1027 komatiite basalts, southeastern Fennoscandia. *Petrology* 13(5), 469-488.
- 1028 Kulikova, V.V., Kulikov, V.S., 1981. New data on Archean peridotitic komatiites in East
 1029 Karelia. *Dokl. Akad. Nauk SSSR.* 259(3), 693-697.
- 1030 Kump, L. R., Brantley, S. L., Arthur, M. A., 2000. Chemical weathering, atmospheric CO₂,
 1031 and climate. *Annu. Rev. Earth Planet. Sci. Lett.* 28, 611-667.
- 1032 Land, M., Ingri, J., Öhlander, B., 1999a. Past and present weathering rates in northern
 1033 Sweden. *Appl. Geochem.* 14, 761-774.
- 1034 Land, M., Öhlander, B., Ingri, J., Thunberg, J., 1999b. Solid speciation and fractionation of
 1035 rare earth elements in a spodosol profile from northern Sweden as revealed by
 1036 sequential extraction. *Chem. Geol.* 160, 121-138.
- 1037 Land, M., Ingri, J., Andersson, P. S., Öhlander, B., 2000. Ba/Sr, Ca/Sr and ⁸⁷Sr/⁸⁶Sr ratios in
 1038 soil water and groundwater: implications for relative contributions to stream water
 1039 discharge. *Appl. Geochem.* 15, 311-325.
- 1040 Land, M., Öhlander, B., 2000. Chemical weathering rates, erosion rates and mobility of major
 1041 and trace elements in a boreal granitic till. *Aquat. Geochem.* 6, 435-460.
- 1042 Land, M., Thunberg, J., Öhlander, B., 2002. Trace metal occurrence in a mineralised and a
 1043 non-mineralised spodosol in northern Sweden. *J. Geochem. Explor.* 75, 71-91.

- 1044 Lavrov, M., 1979. Ultramafic and layered peridotite-gabbro-norite intrusions in Precambrian
1045 in Northern Karelia. Nauka, Leningrad, 135 p.
- 1046 Lesovaya, S., Goryachkin, S., Pogozev, E., Polekhovskii, Y., Zavarzin, A., Zavarzina, A.,
1047 2008. Soils on hard rocks in the Northwest of Russia: Chemical and mineralogical
1048 properties, genesis, and classification problems. *Eurasian Soil Science* 41(4), 363-376.
- 1049 Lesovaya, S., Goryachkin Yu, S.V., Polekhovskii, S., 2012. Soil formation and weathering on
1050 ultramafic rocks in the mountainous tundra of the Rai-Iz massif, Polar Urals. *Eurasian*
1051 *Soil Science* Volume 45, Issue 1, pp 33–44.
- 1052 Li, C., Yang, S., 2010. Is chemical index of alteration (CIA) a reliable proxy for chemical
1053 weathering in global drainage basin? *Am. J. Sci.* 310, 111-127.
- 1054 Lobach-Zhuchenko, S., Levchenkov, O., Cherulaev, V., Krylov, I., 1986. Geological
1055 evolution of the Karelian granite-greenstone terrain. *Precambrian Res.* 33(1-3), 45-65.
- 1056 Lobach-Zhuchenko, S., Chekulayev, V., Sergeev, S., Levchenkov, O., Krylov, I., 1993.
1057 Archaean rocks from southeastern Karelia (Karelian granite greenstone terrain).
1058 *Precambrian Res.* 62(4), 375-397.
- 1059 Lobach-Zhuchenko, S., Arestova, N., Chekulaev, V., Levsky, L., Bogomolov, E., Krylov, I.,
1060 1998. Geochemistry and petrology of 2.40-2.45 Ga magmatic rocks in the north-
1061 western Belomorian Belt, Fennoscandian Shield, Russia. *Precambrian Res.* 92, 223-
1062 250.
- 1063 Louvat, P., Allègre, C. J., 1997. Present denudation rates on the island of Réunion determined
1064 by river geochemistry: Basalt weathering and mass budget between chemical and
1065 mechanical erosions. *Geochim. Cosmochim. Acta* 61(17), 3645-3669.
- 1066 Louvat, P., Allègre, C. J., 1998. Riverine erosion rates on Sao Miguel volcanic island, Azores
1067 archipelago. *Chem. Geol.* 148(3-4), 177-200.
- 1068 Lozovik, P., Potapova, I., 2006. Input of chemical substances with atmospheric precipitation
1069 onto the territory of Karelia. *Water Resour.* 33(1), 104-111.
- 1070 Lundström, U., 1993. The role of organic acids in soil solution chemistry in a podzolized soil.
1071 *J. Soil Sci.* 44, 121-133.
- 1072 Lundström, U. S., van Breemen, N., Bain, D., 2000a. The podzolization process. A review.
1073 *Geoderma* 94, 91-107.
- 1074 Lundström, U. S., van Breemen, N., Bain, D. et al., 2000b. Advances in understanding the
1075 podzolization process resulting from a multidisciplinary study of three coniferous
1076 forest soils in the Nordic Countries. *Geoderma* 94(2-4), 335-353.
- 1077 Maher, K., 2011. The role of fluid residence time and topographic scales in determining
1078 chemical fluxes from landscapes. *Earth Planet. Sci. Lett.*, 312, 48-58.
- 1079 Maher, K., Chamberlain, C.P., 2014. Hydrologic regulation of chemical weathering and the
1080 geologic. *Science*, 343, 1502-1504.
- 1081 Maksimova, M., 1967. Inorganic and organic composition of major ions in rivers of Karelian
1082 coast of the White Sea (in Russian). *Gidrobiologicheskie issledovaniya na Karelskom*
1083 *poberezhie Belogo morya.* Nauka, Leningrad, 9-20.
- 1084 Melkerud, P., Bain, D., Jongmans, A., Tarvainen, T., 2000. Chemical, mineralogical and
1085 morphological characterization of three podzols developed on glacial deposits in
1086 Northern Europe. *Geoderma* 94, 125-148.
- 1087 Meunier, A., Caner, L., Hubert, F., El Alabani, A., Prêt D., 2013. The weathering intensity
1088 scale (WIS) : an alternative approach of the chemical index of alteration. *American*
1089 *Journal of Science*, Vol.313, 113–143.
- 1090 Millot, R., Gaillardet, J., Dupré, B., Allègre, C.J., 2002. The global control of silicate
1091 weathering rates and the coupling with physical erosion: new insights from rivers of
1092 the Canadian Shield. *Earth Planet. Sci. Lett.* 196, 83–98.
- 1093 Millot, R., Gaillardet, J., Dupré, B., Allègre, C. J., 2003. Northern latitude chemical

- 1094 weathering rates: Clues from the Mackenzie River basin, Canada. *Geochim.*
1095 *Cosmochim. Acta* 67(7), 1305-1329.
- 1096 Mokma, D., Yli-Halla, M., Lindqvist, K., 2004. Podzol formation in sandy soils of Finland.
1097 *Geoderma* 120, 259-272.
- 1098 Muir, A., 1961. The podzol and podzolic soils. *Advances in Agronomy* 13, 1-56.
- 1099 Murashkina, M., Southard, R., Pettygrove, G., 2007. Silt and fine sand fractions dominate K
1100 fixation in soils derived from granitic alluvium of the San Joaquin Valley, California.
1101 *Geoderma* 141, 283-293.
- 1102 Nesbitt, H. W., Young, G. M., 1982. Early Proterozoic climates and plate motions inferred
1103 from major element chemistry of lutites. *Nature* 299, 715-717.
- 1104 Öhlander, B., Ingri, J., Ponter, C., 1991. Geochemistry of till weathering in the Kalix River
1105 Watershed, northern Sweden. Reports in forest ecology and forest soils, Swedish
1106 University of Agricultural Sciences. In: *Chemical weathering under field conditions*
1107 (ed. K. Rosén) 63, 1-18.
- 1108 Öhlander, B., Land, M., Ingri, J., Widerlund, A., 1996. Mobility of rare earth elements during
1109 weathering of till in northern Sweden. *Appl. Geochem.* 11, 93-99.
- 1110 Öhlander, B., Thunberg, J., Land, M., Høglund, L. O., Quishang, H., 2003. Redistribution of
1111 trace metals in a mineralized spodosol due to weathering, Liikavaara, northern
1112 Sweden. *Appl. Geochem.* 18, 883-899.
- 1113 Oliva, P., Viers, J., Dupré, B., Fortune, J. P., Martin, F., Braun, J.-J., Nahon, D., Robain, H.,
1114 1999. The effect of organic matter on chemical weathering: Study of a small tropical
1115 watershed: Nsimi-Zoétéélé site, Cameroon. *Geochim. Cosmochim. Acta* 63(23/24),
1116 4013-4035.
- 1117 Oliva, P., Dupré, B., Martin, F., Viers, J., 2004. The role of trace minerals in chemical
1118 weathering in a high-elevation granitic watershed (Estibère, France): Chemical and
1119 mineralogical evidence. *Geochim. Cosmochim. Acta* 68(10), 2223-2244.
- 1120 Olsson, M. T., Melkerud, P., 2000. Weathering in three podzolized pedons on glacial deposits
1121 in northern Sweden and central Finland. *Geoderma* 94, 149-161.
- 1122 Opfergelt, S., Burton, K.W., Georg, R.B., West, A.J., Guicharnaud, R.A., Sigfusson, B.,
1123 Siebert, C., Gislason, S.R., Halliday, A.N., 2014. Magnesium retention on the soil
1124 exchange complex controlling Mg isotope variations in soils, soil solutions and
1125 vegetation in volcanic soils, Iceland. *Geochim. Cosmochim. Acta* 125, 110-130.
- 1126 Parry, S.A., Hodson, M.E., Kemp, S.J., Oelkers, E.H., 2015. The surface area and reactivity
1127 of granitic soils: I. Dissolution rates of primary minerals as a function of depth and age
1128 deduced from field observations. *Geoderma* 237-238, 21-35.
- 1129 Peuraniemi, V., Aario, R., Pulkkinen, P., 1997. Mineralogy and geochemistry of the clay
1130 fraction of till in northern Finland. *Sedimentary Geology* 111, 313-327.
- 1131 Pokrovsky, O.S., Schott, J., 2002. Iron colloids/organic matter associated transport of major
1132 and trace elements in small boreal rivers and their estuaries (NW Russia). *Chem. Geol.*
1133 190, 141-179.
- 1134 Pokrovsky, O.S., Schott, J., Kudryavtsev, D. I., Dupré, B., 2005. Basalt weathering in Central
1135 Siberia under permafrost conditions. *Geochim. Cosmochim. Acta* 69(24), 5659-5680.
- 1136 Pokrovsky, O. S., Schott, J., Dupré, B., 2006a. Trace element fractionation and transport in
1137 boreal rivers and soil porewaters of permafrost-dominated basaltic terrain in Central
1138 Siberia. *Geochim. Cosmochim. Acta* 70, 3239-3260.
- 1139 Pokrovsky, O.S., Schott, J., Dupré, B., 2006b. Basalt weathering and trace elements migration
1140 in the boreal Arctic zone. *J. Geochem. Explor.* 88, 304-307.
- 1141 Ponomareva, V., 1964. Theory of podzol-formation process (in Russian). M.-L.: Nauka, p.
1142 380.
- 1143 Puchtel, I., Hofmann, A., Mezger, K., Shchipansky, A., Kulikov, V., Kulikova, V., 1996.

- 1144 Petrology of a 2.41 Ga remarkably fresh komatiitic basalt lava lake in Lion Hills,
1145 central Vetreny Belt, Baltic Shield. *Contrib. Mineral. Petrol.* 124(3-4), 273-290.
- 1146 Puchtel, I. S., Haase, K. M., Hofmann, A. W., Chauvel, C., Kulikov, V. S., Garbe-Schonberg,
1147 C., Nemchin, A. A., 1997. Petrology and geochemistry of crustally contaminated
1148 komatiitic basalts from the Vetreny Belt, southeastern Baltic Shield: Evidence for an
1149 early Proterozoic mantle plume beneath rifted Archean continental lithosphere.
1150 *Geochim. Cosmochim. Acta* 61(6), 1205-1222.
- 1151 Raymon, P.A., 2017. Temperature versus hydrological controls of chemical weathering fluxes
1152 from United States forests. *Chem. Geol.* 458, 1-13.
- 1153 Reimann, C., Melezhik, V., 2001. Metallogenic provinces, geochemical provinces and
1154 regional geology - what causes large-scale patterns in low density geochemical maps
1155 of the C-horizon of podzols in Arctic Europe? *Appl. Geochem.* 16(7-8), 963-983.
- 1156 Remaury, M., Oliva, P., Guillet, B., Martin, F., Toutain, F., Dagnac, J., Belet, J., Dupré, B.,
1157 Gauquelin, T., 2002. Nature and genesis of spodic horizons characterized by inverted
1158 color and organic content in a subalpine podzolic soil (Pyrenees Mountains, France).
1159 *Bulletin de la Société Géologique de France* 172(1), 77-86.
- 1160 Revyako, N., Bychkova, Y., Kostitsyn, Y., 2007. Isotope evidence of the interaction of basic
1161 melt with crust rocks on the example of Kivakka layered intrusion (Karelia) (in
1162 Russian). *Proceedings of International conference "Ultrabasic-basic complexes of fold
1163 regions"*. Irkutsk, 487-490.
- 1164 Riebe, C. S., Kirchner, J. W., Granger, D. E., Finkel, R. C., 2001 Strong tectonic and weak
1165 climatic control of long-term chemical weathering rates. *Geology* 29, 511-514.
- 1166 Riebe, C. S., Kirchner, J. W., Finkel, R. C., 2004. Erosional and climatic effects on long-term
1167 chemical weathering rates in granitic landscapes spanning diverse climate regimes.
1168 *Earth Planet. Sci. Letters* 224, 547-562.
- 1169 Righi, D., Chauvel, A., 1987. Podzols and Podzolization. *Assoc. Franc. Etude Sol. INRA,*
1170 *Plaisir et Paris, Paris.*
- 1171 Ryabchikov, I., Suddaby, P., Giris, A., Kulikov, V., Kulikova, V., Bogatkov, O., 1988.
1172 Trace-element geochemistry of Archaean and Proterozoic rocks from eastern Karelia,
1173 USSR. *Lithos* 21, 183-194.
- 1174 Salminen, R., Gregorauskiene, V., Tarvainen, T., 2008. The normative mineralogy of 10 soil
1175 profiles in Fennoscandia and north-western Russia. *Appl. Geochem.* 23(12), 3651-
1176 3665.
- 1177 Sarala, P., 2005. Till geochemistry in the ribbed moraine area of Peräpohjola, Finland. *Appl.*
1178 *Geochem.* 20, 1714-1736.
- 1179 Sawhney, B.L., 1989. Minerals in soil environments. *Soil Science Society of America,*
1180 *chapter 16: Interstratification in layer silicates, 789-828.*
- 1181 Schopka, H., Derry, L., Arcilla, C., 2011. Chemical weathering, river geochemistry and
1182 atmospheric carbon fluxes from volcanic and ultramafic regions on Luzon Island, the
1183 Philippines. *Geochim. Cosmochim. Acta* 75, 978-1002. Schopka, H., Derry, L., 2012.
1184 Chemical weathering fluxes from volcanic islands and the importance of groundwater:
1185 The Hawaiian example. *Earth and Planetary Science Letters* 339-340, 67-78.
- 1186 Schroeder, P.A., Melear, N.D., West, L.T., Hamilton, D.A., 2000. Meta-gabbro weathering in
1187 the Georgia Piedmont, USA: implications for global silicate weathering rates. *Chem.*
1188 *Geol.* 163, 235-245.
- 1189 Schweda, P., Araujo, P. D. R., Sjoeborg, L., 1991. Soil chemistry, clay mineralogy and
1190 noncrystalline phases in soil profiles from southern Sweden and Gårdsjön.. In: Rosén,
1191 K. (Ed.), *Chemical weathering under field conditions. Reports in Forest Ecology and
1192 Forest Soils.* Swedish University of Agricultural Sciences 63, 49-62.
- 1193 Semenov, V., Koptev-Dvornikov, E., Berkovskii, A., Kireev, B., Pchelintseva, N., Vasil'eva,

- 1194 M., 1995. Layered troctolite-gabbro-norite Tsippinga intrusion, Northern Karelia:
1195 Geologic structure and petrology. *Petrology* 3(6), 588-610.
- 1196 Shmygalev, V., 1968. Mafic and ultramafic intrusions of the Olanga group. Proterozoic
1197 volcanic and ultramafic complexes of Karelia 1, 209-219.
- 1198 Simonsson, M., Bergholm, J., Olsson, B.A., von Brömssen, C., Öborn, I., 2015. Estimating
1199 weathering rates using base cation budgets in a Norway spruce stand on podzolised
1200 soil: Analysis of fluxes and uncertainties. *Forest Ecol. Management*, 340, 135-152.
- 1201 Starr, M., Lindroos, A., Ukonmaanaho, L., Tarvainen, T., Tanskanen, H., 2003. Weathering
1202 release of heavy metals from soil in comparison to deposition, litterfall and leaching
1203 fluxes in a remote, boreal coniferous forest. *Appl. Geochem.* 18, 607-613.
- 1204 State Geological Map of Russian Federation, 2001. In: Bogdanov, Yu.B. (Ed.), *Explication*
1205 *Note*. Ministry of Natural Resources, St-Petersbourg, VSEGEI. Sheet Q-(35)-37.
- 1206 Sun, X., Mörth, C.-M., Humbord, C., Gustafsson, B., 2017. Temporal and spatial variations of
1207 rock weathering and CO₂ consumption in the Baltic Sea catchment. *Chem. Geol.* 466,
1208 57-69.
- 1209 Stroeven, A.P., Hättestrand, C., Kleman, J., Heyman, J., Fabel, D., Fredin, O., Goodfellow,
1210 B.W., Harbor, J.M., Jansen, J.D., Olsen, L., 2016. Deglaciation of Fennoscandia.
1211 *Quaternary Sci. Rev.* 147, 91-121.
- 1212 Taylor, S., McLennan, S., 1985. *The continental crust: its composition and evolution*.
1213 Blackwell Scientific Publications, Oxford, p. 312.
- 1214 Thiede, J., Bauch, H. A., Hjort, C., Mangerud, J., 2001. The late Quaternary stratigraphy and
1215 environments of northern Eurasia and the adjacent Arctic seas - new contributions
1216 from QUEEN. *Global and Planetary Change* 31(1-4), vii-x.
- 1217 Thorn, C.E., Dixon, J.C., Darmody, R.G., Allen, C.E., 2006. A 10-year record of the
1218 weathering rates of surficial pebbles in Kärkevagge, Swedish Lapland. *Catena* 65,
1219 272-278.
- 1220 Tyler, G., 2004. Vertical distribution of major, minor, and rare elements in a Haplic Podzol.
1221 *Geoderma* 119, 277-290.
- 1222 Vasiliev, M.V., 2006. Specific features of Vetreny Belt paleorift intrusive systems (in
1223 Russian). M.Sc. thesis, Faculty of Geology, Moscow State University.
- 1224 Vasyukova, E., Pokrovsky, O.S., Viers, J., Oliva, P., Dupré, B., Martin, F., Candaudap, F.,
1225 2010. Trace elements in organic- and iron-rich surficial fluids of boreal zone:
1226 Assessing colloidal forms via dialysis and ultrafiltration. *Geochim. Cosmochim. Acta*
1227 74, 449-468.
- 1228 Viers, J., Dupré, B., Braun, J., Deberdt, S., Angeletti, B., Ngoupayou, J. N., Michard, A.,
1229 2000. Major and trace element abundances, and strontium isotopes in the Nyong basin
1230 rivers (Cameroon): constraints on chemical weathering processes and elements
1231 transport mechanisms in humid tropical environments. *Chem. Geol.* 169, 211-241.
- 1232 Wymore, A.S., Brereton, R.L., Ibarra, D.E., Maher, K., McDowell, W.H., 2017. Critical zone
1233 structure controls concentration-discharge relationships and solute generation in
1234 forested tropical montane watersheds. *Water Resources Res.*, 53(7), 6279-6295.
- 1235 World reference base for soil resources (IUSS Working Group WRB, FAO), 2006.
- 1236 Zakharova, E., Pokrovsky, O. S., Dupré, B., Gaillardet, J., Efimova, L., 2007. Chemical
1237 weathering of silicate rocks in Karelia region and Kola peninsula, NW Russia:
1238 Assessing the effect of rock composition, wetlands and vegetation. *Chem. Geol.* 242,
1239 255-277.
- 1240 Zilliacus, H., 1989. Genesis of De Geer moraines in Finland. *Sediment. Geol.* 62(2-4), 309-
1241 317.
- 1242

1243
1244
1245
1246

Table 1. Soils and surface waters studied and their bedrock composition. Sample series from Vetreny Belt paleorift and Kivakka intrusion are defined as "V" and "K", respectively. Samples marked with "w" correspond to surface waters and with "ss" - to soil solutions.

1247

Sample no.	Description	Bedrock composition
<u>Soils</u>		
V-4	Podzol	Komatiitic basalts, glacial deposits
V-7	Podzol	Komatiitic basalts, glacial deposits
V-9	Regosol	Gneisses, glacial deposits
V-15	Regosol	Peridotites
V-16	Podzol	Gneisses, glacial deposits
K-7	Podzol	Gneisses, glacial deposits
K-8	Podzol	Gneisses, glacial deposits
K-14	Podzol	Olivinite
K-29	Regosol	Gneisses, glacial deposits
K-37	Podzol	Gabbro-norites
<u>Waters</u>		
V-3-w	Surface water	Basalt
V-9-w	r. Ruiga	Basalt
V-10-w	Surface water from basalt field	Basalt
V-11-w	Surface water from basalt field	Basalt
V-12-w	r. Ruiga, upstream biofilms	Basalt
V-13-w	r. Ruiga, highest upstream	Basalt
V-15-w	Creek over ultramafites	Ultramafites
V-18-w	r. Nukcha	Basalt
K-7-w	r. Palajoki, tributary	Gneisses, glacial deposits
K-8-w	Subsurface flow (right bank of the r. Palajoki)	Gneisses, glacial deposits
K-10-w	Swamp (corresponds to K-43 and K-44)	Gabbro-norites
K-12-w	Spring from a swamp	Gneisses, glacial deposits
K-13-w	River over olivenites	Olivinite
K-17-w	Subsurface flow	Norites
K-30-w	r. Vartalambina downstream	Gneisses, glacial deposits
K-31-w	r. Vartalambina upstream, tributary	Gneisses, glacial deposits
K-32-w	Swamp	Gabbro-norites
K-33-w	Stream	Gabbro-norites
K-38-w	Swamp	Gabbro-norites
K-39-w	Swamp	Gabbro-norites
K-41-w	r. Molodilny (springing from swamp)	Gabbro-norites
K-43-w	Swamp	Gabbro-norites
K-44-w	Swamp	Gabbro-norites
K-45-w	r. Palajoki	Gneisses, glacial deposits
<u>Soil solutions</u>		
V-16-ss	Soil water	Peridotites, olivinites
K-5-ss	Soil solution	Gabbro-norites
K-35-ss	Soil solution	Norites

1248

Table 2. Major, trace elements ($\mu\text{g L}^{-1}$) and dissolved organic carbon (DOC) concentrations, and strontium isotopic ratios ($^{87}\text{Sr}/^{86}\text{Sr}$) measured in the dissolved phase (i. e. < 0.22 (0.45) μm) in river and swamp waters from Vetreny Belt (sampled on 12-23 July 2004) and Kivakka intrusion zone (sampled on 10-19 July 2006). “nm” stands for not measured; “<dl” – below detection limit; “TDS” – total dissolved solids; “RW” – river water; “SW” – surface water; “SWW” – mire water; “SS” – soil solution; γ – felsic substratum; β – basaltic substratum; G-n – gabbro-norite; N – norite; Ol – olivinite; P – peridotite.

<u>Vetreny Belt</u>	<u>V-9-w</u>	<u>V-12-w</u>	<u>V-13-w</u>	<u>V-15-w</u>	<u>V-18-w</u>	<u>V-10-w</u>	<u>V-11-w</u>	<u>V-3-w</u>	<u>V-16-sw</u>
0.22 μm	RW	RW	RW	RW	RW	SW	SW	SW	SS
$\mu\text{g/l}$	β	β	β	P	β	β	β	β	P
pH	5.92	5.9	6.5	5.07	7.05	5.18	5.18	5.46	7.11
t°C	20	27	27	25	23	29	29	23	24
DOC, mg/l	36.5	34.7	35.7	39.7	17.2	8.8	98.5	9.8	20.6
Na ⁺	2 335	2 532	2 215	1 687	4 430	1 800	2 045	1 365	1 508
K ⁺	514	469	407	106	224	517	304	305	651
Mg ²⁺	2 867	2 793	6 034	3 128	2 917	425	328	544	8 023
Ca ²⁺	1 838	1 811	1 689	837	2 943	1 296	922	1 112	516
H ₄ SiO ₄	4 900	5 070	4 030	4 020	2 210	3 970	4 540	2 930	5 980
Cl ⁻	1 270	nm	1 590	2 080	3 900	1 582	2 460	1 350	2 210
SO ₄ ²⁻	750	nm	531	531	800	900	810	1 540	1 590
NO ₃ ⁻	<dl	<dl	480	295	101	100	<dl	290	539
F ⁻	70	<dl	<dl	39	56	28	<dl	33	<dl
[Alk], mg/l	4.85	5.56	16.6	2.05	28	4.21	4.84	1.77	29.89
Al	nm	537	340	319	56	264	310	244	161
Fe	1 888	865	752	2 374	2 216	618	135	290	311
Rb	0.52	0.59	0.53	0.38	0.48	0.85	0.41	0.56	0.76
Sr	13.00	12.18	11.19	5.08	18.81	11.99	9.24	10.11	4.15
TDS, mg/l	16.4	14.1	18.1	15.4	19.9	11.5	8.6	10.0	21.5
$^{87}\text{Sr}/^{86}\text{Sr}$	0.723799 ± 20	nm	nm	0.722741 ± 20	0.721984 ± 12	nm	nm	0.715087 ± 17	0.723249 ± 33

Table 2, continued.

Kivakka intrusion	K-7-w	K-8-w	K-12-w	K-30-w	K-31-w	K-45-w	K-13-w	K-17-w	K-33-w
0.45 μm	RW	RW	SW	RW	RW	RW	RW	SW	RW
$\mu\text{g/l}$	γ	γ	γ	γ	γ	γ	OI	N	G-n
pH	7.36	5.95	6.56	7.42	7.45	7.31	6.56	6.72	6.13
t°C	16	6	nm	nm	nm	nm	nm	nm	nm
DOC, mg/l	10.42	1.74	5.60	6.32	5.08	94.36	30.55	2.22	6.41
Na ⁺	1 667	1 379	2 161	2 732	1 714	1 652	1 378	2 044	1 164
K ⁺	502	315	64	386	907	370	374	72	38
Mg ²⁺	2 106	674	1 451	3 898	7 874	1 821	13 002	1 218	570
Ca ²⁺	9 745	2 047	4 891	10 596	17 435	7 219	1 901	7 385	2 328
H ₄ SiO ₄	3 210	3 990	3 760	4 880	3 290	2 390	7 310	4 560	3 200
Cl ⁻	568	576	295	393	495	526	453	534	400
SO ₄ ²⁻	1 498	3 650	2 300	351	688	1 922	432	3 576	736
NO ₃ ⁻	<dl	<dl	<dl	<dl	139	<dl	<dl	<dl	<dl
F ⁻	<dl	<dl	<dl	<dl	<dl	<dl	<dl	<dl	<dl
[Alk], mg/l	27.38	8.28	22.76	39.42	80.20	28.32	40.21	26.17	9.59
Al	26.34	32.30	51.74	7.48	9.76	32.97	191.38	20.07	125.24
Fe	2 589.87	5.59	116.64	115.31	246.79	2 124.46	391.96	3.33	270.26
Rb	1.23	0.99	0.17	0.78	1.79	1.06	1.53	0.20	0.15
Sr	50.89	9.94	12.55	17.20	15.91	36.96	14.26	14.79	8.50
TDS, mg/l	19.30	12.63	14.92	23.24	32.54	15.90	24.85	19.39	8.44
⁸⁷ Sr/ ⁸⁶ Sr	0.721067 ± 15	0.725299 ± 15	0.716615 ± 15	nm	nm	0.721102 ± 12	0.717867 ± 21	0.713467 ± 19	nm

Table 2, continued.

Kivakka intrusion	K-41-w	K-10-w	K-43-w	K-44-w	K-32-w	K-38-w	K-39-w	K-5-ss	K-35-ss
0.45 µm	RW	SWW	SWW	SWW	SWW	SWW	SWW	SS	SS
µg/l	G-n	γ	G-n	G-n	G-n	G-n	G-n	N	G-n
pH	7.17	4.94	5.85	5.41	4.56	4.65	5.03	4.94	nm
t°C	nm	24	16	21	nm	19	nm	6	nm
DOC, mg/l	4.96	29.46	nm	31.59	16.65	11.60	5.28	3.43	40.34
Na ⁺	1 871	1 031	1 094	1 068	1 399	845	743	569	1 102
K ⁺	89	58	32	50	190	249	133	77	178
Mg ²⁺	1 068	832	1 327	1 055	384	217	165	114	674
Ca ²⁺	3 166	2 065	3 707	2 382	909	644	674	520	1 305
H ₄ SiO ₄	3 700	1 930	2 780	2 250	2 470	490	760	2 520	4 540
Cl ⁻	374	725	726	841	1 252	1 180	742	217	1 414
SO ₄ ²⁻	1 610	494	255	235	332	220	599	1 853	1 868
NO ₃ ⁻	<dl	<dl	<dl	<dl	<dl	<dl	<dl	862	595
F ⁻	<dl	<dl	<dl	<dl	<dl	<dl	<dl	<dl	<dl
[Alk], mg/l	16.61	nm	8.06	2.67	2.20	2.76	2.72	1.77	nm
Al	42.69	453.75	302.11	386.37	163.85	179.22	224.63	274.24	440.35
Fe	36.68	3 876.17	10 507.70	4 778.12	164.02	180.11	237.39	913.91	41.37
Rb	0.17	0.10	0.13	0.08	0.51	0.45	0.24	0.29	0.65
Sr	11.56	12.93	16.71	14.19	4.09	4.02	5.31	3.65	10.44
TDS, mg/l	11.88	11.5	20.7	13.0	7.3	4.2	4.3	7.9	12.2
⁸⁷ Sr/ ⁸⁶ Sr	0.713984 ± 13	nm	0.721347 ± 46	nm	nm	nm	nm	nm	nm

Table 3. Mineralogical composition of studied soils. Number of “+” signs indicates different degree of presence of a mineral in soil, “Tr.” stands for “traces”. Empty cells correspond to the absence of a mineral in the soil sample.

Mineral composition	Quartz	Feldspar	Amphibole	Illite	Vermiculite	Chlorite	Hydrobiotite	Amorphous phases	Interlayered Mica/Vermiculate	Smectite	Talc
K-7-B	+	++	+	+	++	Tr.					
K-14-B1	Tr.			+	+++	+					
K-14-C			+	+	+++	+					Tr.
K-29-O/A	++	++	+	++		Tr.	++	+	+		
K-29-E	++	++	Tr.	++		Tr.	++	+			
K-37-A	++	++	++	++							
K-37-B1	++	++	+	+	++	+				+	
K-37-B2	++	+	+	+	+	+					
V-16-E	++	++	++	+				++			
V-16-B	++	++	+	+	+			+			
V-4-E	++	+	Tr.	Tr.		+				++	
V-7-B	++	+	+	+	+	++		+			
V-9-A	++	+	+					+			
V-15-O/A			+	+	++					++	

Table 4. Chemical Depletion Fraction (CDF), Chemical Depletion Fraction of individual element (CDFx), Chemical Index of Alteration (CIA), CIA_{soil}/CIA_{rock} ratios and poles (4Si, R^{2+} and M+) calculations for the Weathering Intensity Scale (WIS) diagram. CDF and CDFx were calculated according to Riebe et al. (2004). CIA values were calculated following Nesbitt and Young (1982) considering that all CaO content are coming from silicate phases. WIS poles were established using the reference study of Meunier et al., 2014 by considering monocationic millimoles from oxide amounts : $4Si = mMol Si/4$; $R^{2+} = mMol Mg^{2+} + mMol Mn^{2+}$; $M^+ = mMol Na^+ + mMol K^+ + 2x mMol Ca^{2+}$. The R^{2+} component was calculated without considering Fe^{2+} content because only total Fe was measured during chemical analyses.

SAMPLE	type of rock	Chemical depletion	Calculated chemical depletion fraction of elements, Ti as invariant								CIA	CIAsoil/CIArock	SOIL WIS		
			% Si	% Al	% Fe	% Ca	% Mg	% Na	% K	% Mn			% 4Si	% M+	% R2+
soil samples															
K-7 E	γ	51%	0,3	0,6	0,9	0,9	1,0	-0,1	-3,8	0,9	50	1,01	54,96	41,76	3,27
K-7 B	γ	52%	0,3	0,7	0,7	0,9	0,9	0,0	-3,0	0,9	50	1,01	52,57	40,68	6,74
K-8 E	γ	2%	-0,1	0,3	0,5	0,7	0,4	0,1	-0,3	0,8	50	1,00	56,13	39,22	4,65
K-8 B	γ	-72%	-0,6	-0,2	-0,6	0,3	-0,2	-0,3	-0,7	0,6	54	1,08	54,26	39,90	5,84
K-8 C	γ	-29%	-0,4	0,1	0,2	0,4	-0,2	-0,3	-0,6	0,6	48	0,98	52,28	41,45	6,26
K-14 B1	Ol	63%	0,6	0,6	0,6	0,7	0,7	0,6	0,6	0,6	46	1,17	14,87	6,25	78,88
K-14 B2	Ol	81%	0,7	0,2	1,0	0,8	1,0	-1,0	-1,5	1,0	48	1,21	50,93	37,13	11,94
K-14 C	Ol	32%	0,3	0,4	0,3	0,4	0,3	0,7	0,9	0,3	42	1,06	13,91	5,14	80,95
K-29 O/A	γ	-520%	-0,5	-0,3	0,2	-0,1	0,2	-0,9	0,5	0,6	45	0,91	46,39	50,59	3,01
K-29 C	γ	-48%	-0,6	-0,3	0,5	-0,1	0,6	-0,9	0,6	0,7	49	0,98	48,03	48,26	3,70
K-29 E	γ	-51%	-0,4	-0,1	0,4	-0,3	0,4	-0,5	0,2	0,1	49	0,99	50,86	47,47	1,66
K-37 O	G-n	6%	0,3	0,6	0,7	0,9	0,9	0,1	-3,2	0,9	49	1,24	53,02	38,82	8,16
K-37 A	G-n	40%	0,3	0,6	0,7	0,9	0,9	0,0	-3,7	0,9	50	1,26	51,80	40,10	8,10
K-37 B1	G-n	33%	0,1	0,6	0,7	0,9	0,9	-0,2	-4,0	0,8	49	1,24	51,34	39,78	8,88
K-37 B2	G-n	23%	0,0	0,4	0,6	0,8	0,8	-0,4	-4,4	0,8	51	1,27	47,38	43,45	9,17
K-37 C	G-n	6%	-0,2	0,3	0,7	0,8	0,8	-0,8	-6,0	0,8	52	1,31	51,66	41,16	7,18
V4 E	β	-65%	-1,7	-0,1	0,9	0,8	1,0	-1,3	-4,9	0,8	52	1,34	66,07	30,71	3,22
V7 E	β	-51%	-1,1	-0,3	0,8	0,7	0,9	-1,3	-5,3	0,8	52	1,35	55,26	37,69	7,05
V7 B	β	-50%	-1,1	-0,4	0,5	0,7	0,8	-1,4	-5,1	0,6	53	1,38	49,09	35,88	15,03
V9 O	γ	-1671%	0,3	0,4	-0,3	-1,0	-0,8	0,6	-0,5	-1,4	32	0,65	25,83	54,88	19,29
V9 A	γ	15%	0,3	0,6	0,1	0,1	-0,8	0,7	0,7	0,4	37	0,75	38,45	37,11	24,44
V16 E	γ	-102%	-1,4	-0,3	0,6	0,2	0,5	-0,8	-1,2	0,7	51	1,02	59,71	36,35	3,94
V16 B	γ	-191%	-2,4	-1,2	-0,2	-0,2	-0,3	-1,8	-2,2	0,2	51	1,03	54,80	37,84	7,36
V15 O/A	P	-123%	-0,8	0,1	-0,9	-0,6	-2,5	0,5	0,5	-2,6	28	0,73	15,67	23,64	60,69
Rock samples															
Goletz Basalt											39		22,44	42,57	35,00
Gabbro-norite											40		22,88	51,73	25,39
TTG											50		43,63	49,91	6,46
Olivenite											40		13,48	6,15	80,37

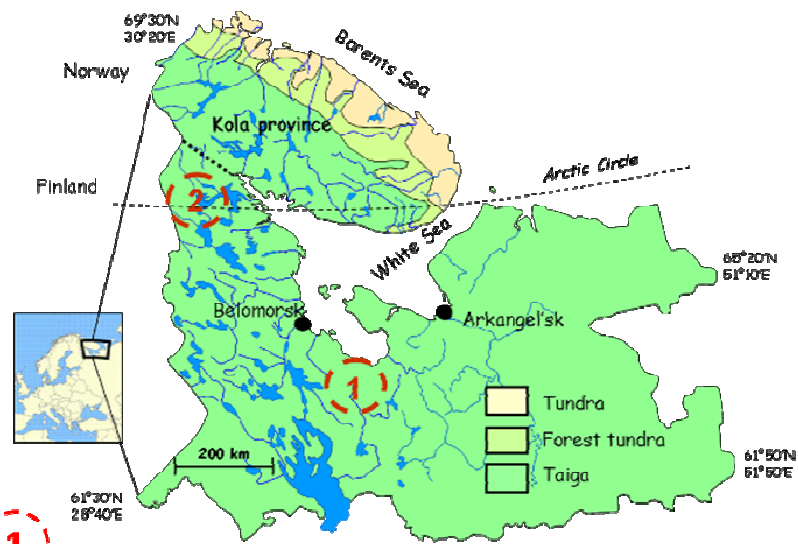
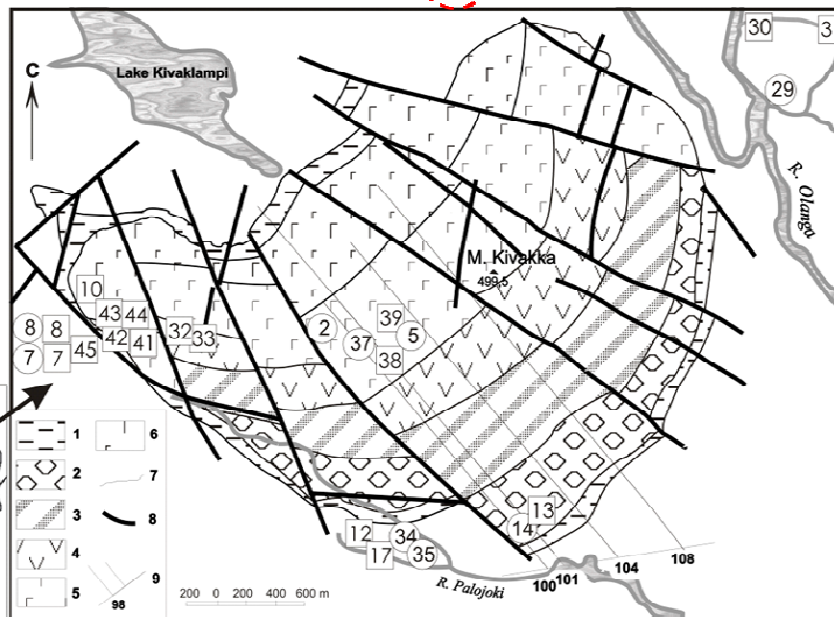
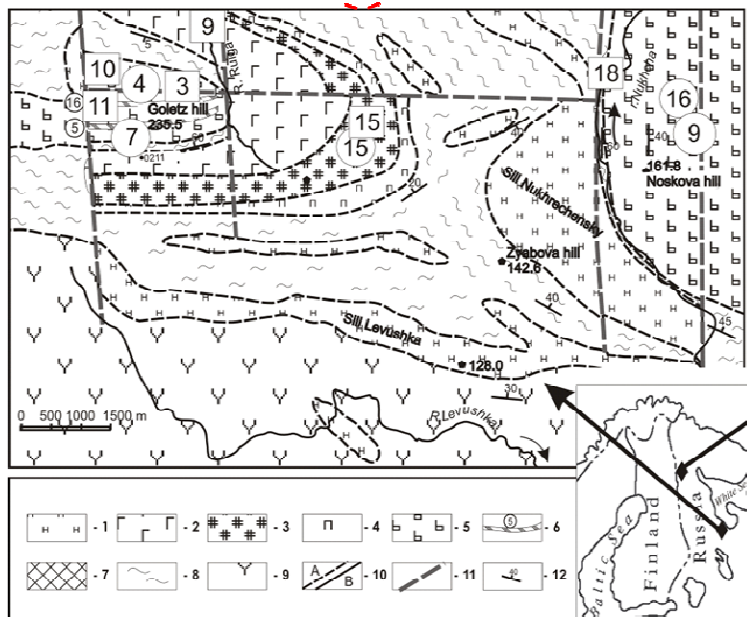


Fig. 1. Map of the studied areas Vetreny Belt paleorift (1) and Kivakka intrusion (2) showing soil (circles) and water (squares) sampling points and geological situation.

1

2



I. Schematic geological map of the Vetreny Belt (from Goletz hill to r. Nukhcha):

1 - nonsegmented mafit-ultramafit sills and dykes, 2 - gabbros, 3 - peridotites, 4 - pyroxenites, 5 - nonsegmented komatiitic basalts, 6 - differentiated covers 5 and 16 (in circles), 7 - probable supplying and deferent canals for prevolcanic camera Ruiga, 8 - Vileng suite sediments, 9 - Kirich suite vulcanites, 10 - geological borders (A - supposed, B - observed), 11 - faults, 12 - deposition elements.

Sample points and their numbers are marked with circles (soils) and squares (water).

Modified after Kulikov et al. (2008).

II. Schematic geological map of the Kivakka intrusion:

1 - Lower and Upper Contact Zones (LCZ and UCZ, respectively), 2 - Olivinite Zone (OZ), 3, 4 - Norite Zone (NZ), 3 - Subzone of Intercalating Bronzites and Norites (SIBN), 5 - Gabbro-Norite Zone (GNZ), 6 - Zone of Gabbro-Norites with Pigeonite (ZGNp), 7 - geological borders, 8 - faults, 9 - profiles of YUKE PGO Sevzapegeologiya.

Sample points and their numbers are marked with circles (soil) and squares (water).

Modified after Bychkova and Koptev-Dvornikov (2004).

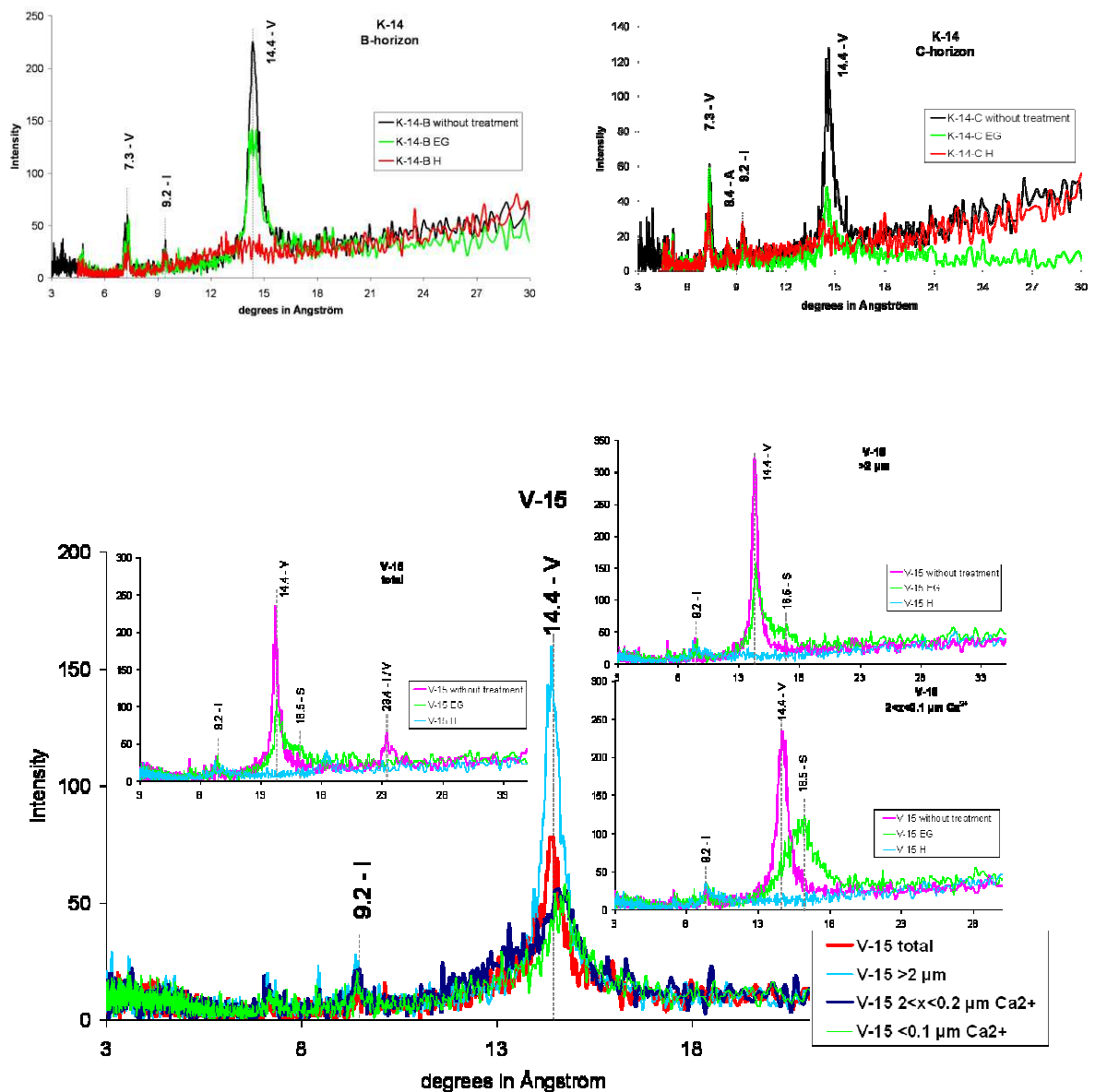


Fig. 2A. Representative X-ray diffractograms of soil profiles K-14 (upper panels) and V-15 (bottom panels). Minerals: I – illite, I/V – interstratified layers of illite and smectite, S – smectite, V – vermiculite. EG – ethylene-glycol saturation, H – heating, Ca²⁺ - calcium saturation.

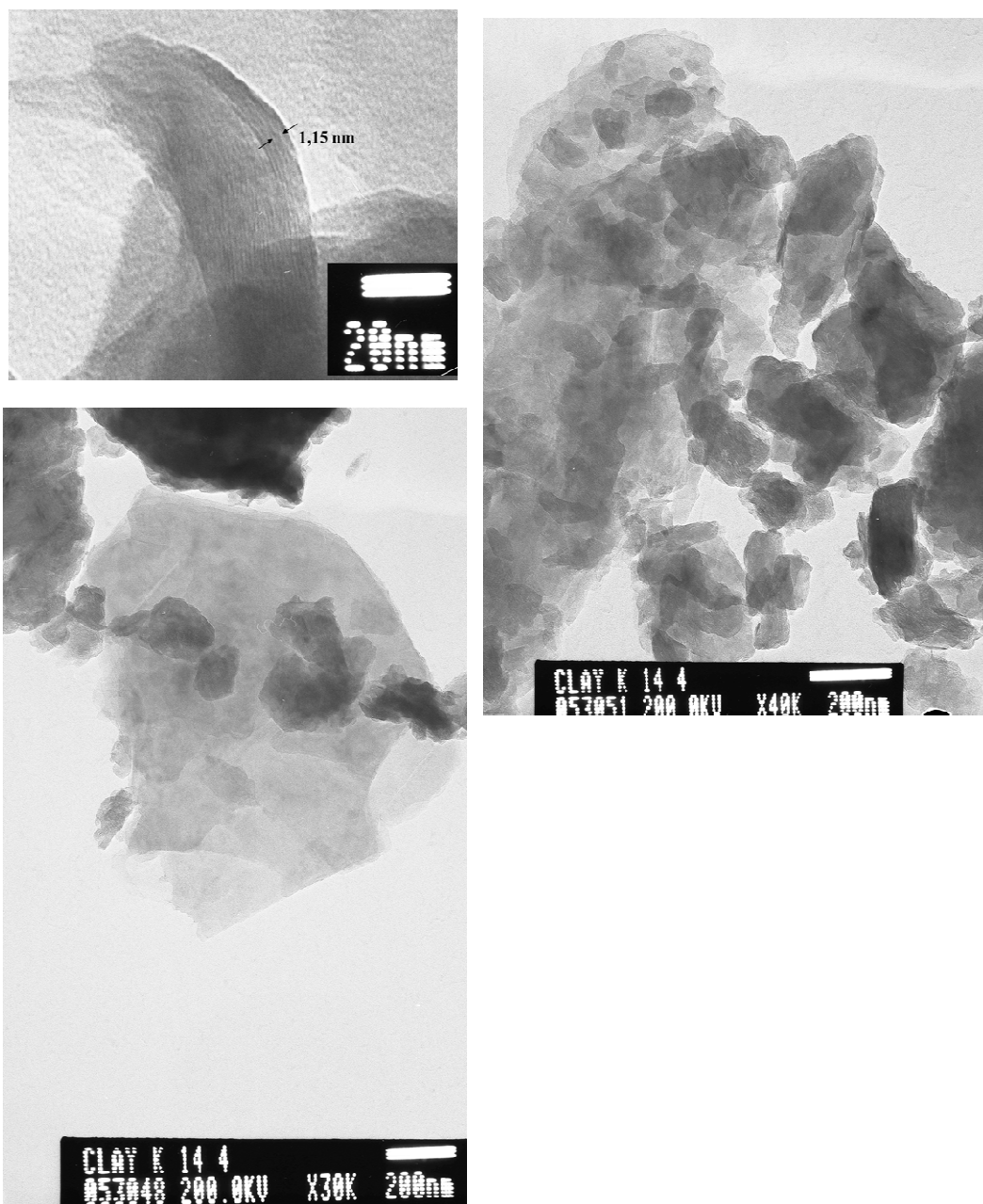


Fig. 2B. Transmission electron microscopy of clays in sample K-14.

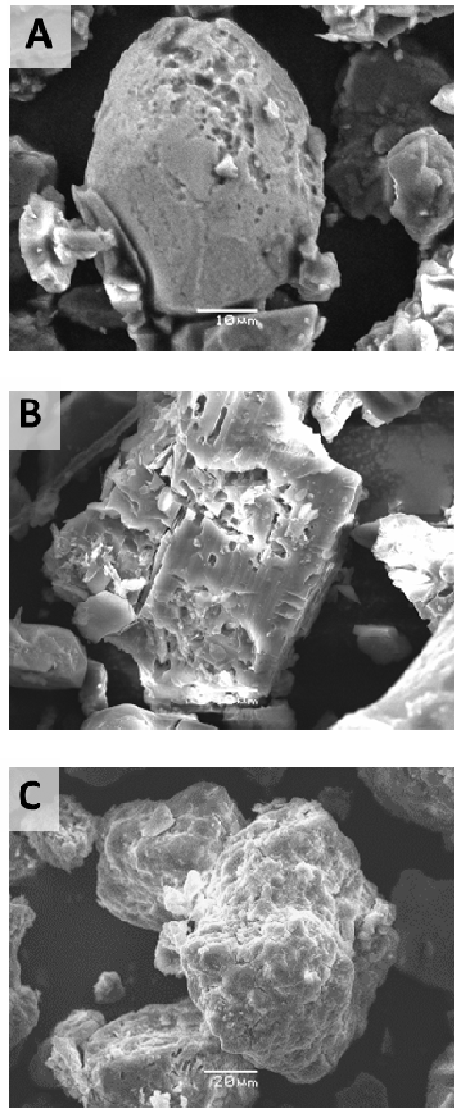


Fig. 3. SEM images of minerals found in soils illustrating neo-formed material and erosion on the surface of minerals: **A**, altered zircon in podzol V-16 over granite; **B**, altered feldspar in regosol K-29 over granite; **C**, quartz covered with aluminous coating in podzol K-37 over gabbro-norite.

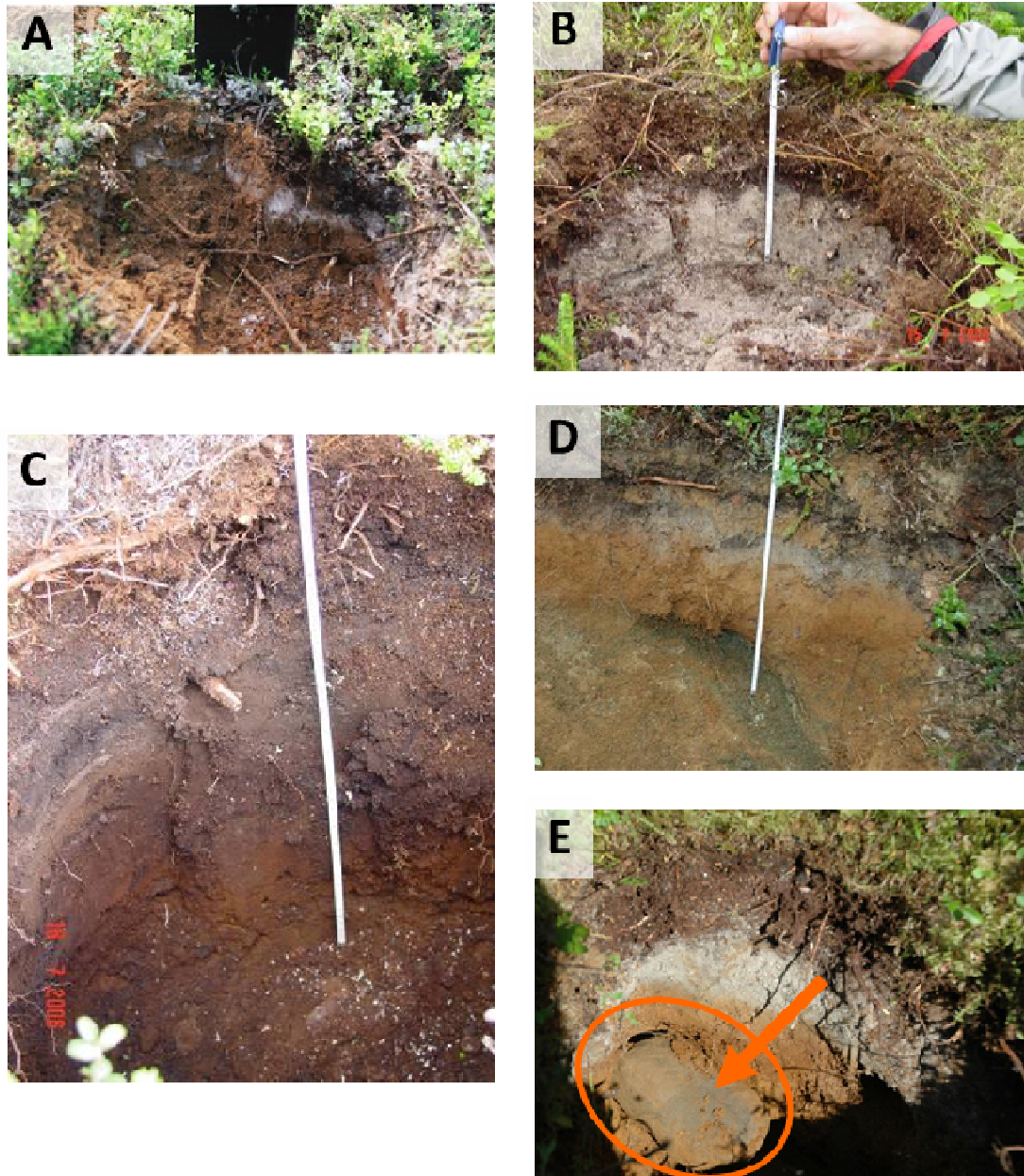


Fig. 4. Photos of podzol V-4 developed on komatiitic basalts from the Goletz hill of Vetreny Belt (A); the regosol K-29 under heather and bilberry bushes developed on gneiss from the Kivakka intrusion zone (B); the podzol K-37 developed on gabbro-norite rock of the Kivakka intrusion (C); the podzol K-14 developed on olivinite rock of the Kivakka intrusion (D) and podzol (K-7) developed on gneiss from the Kivakka intrusion zone (E). Full scale quaternary (Pleistocene) deposits can be observed in the deepest horizon confirming a strong moraine influence in this region.

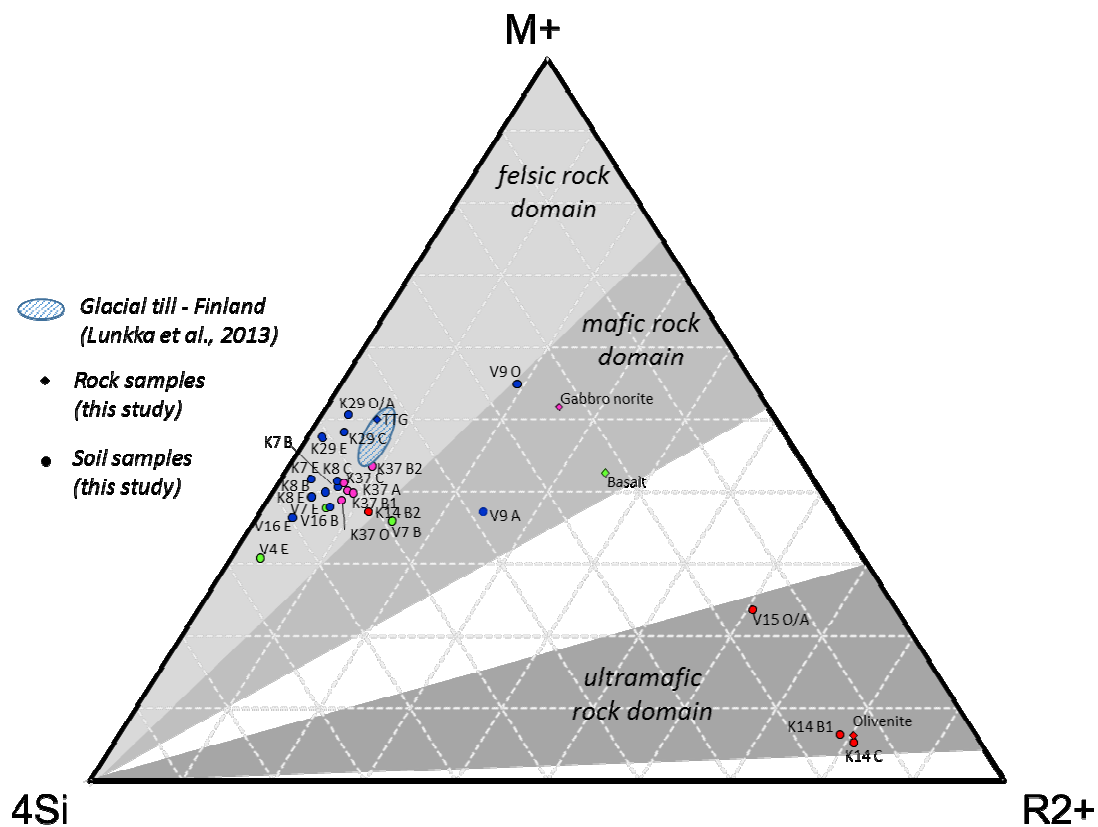


Fig. 5. WIS diagram including all the studied soil samples, Olivinite, Gabbro-norite, TTG rocks from Kivakka, Goltetz Basalt from Vetreny Belt and glacial till from Finland (Lunkka et al., 2013). See table 4 for calculations.

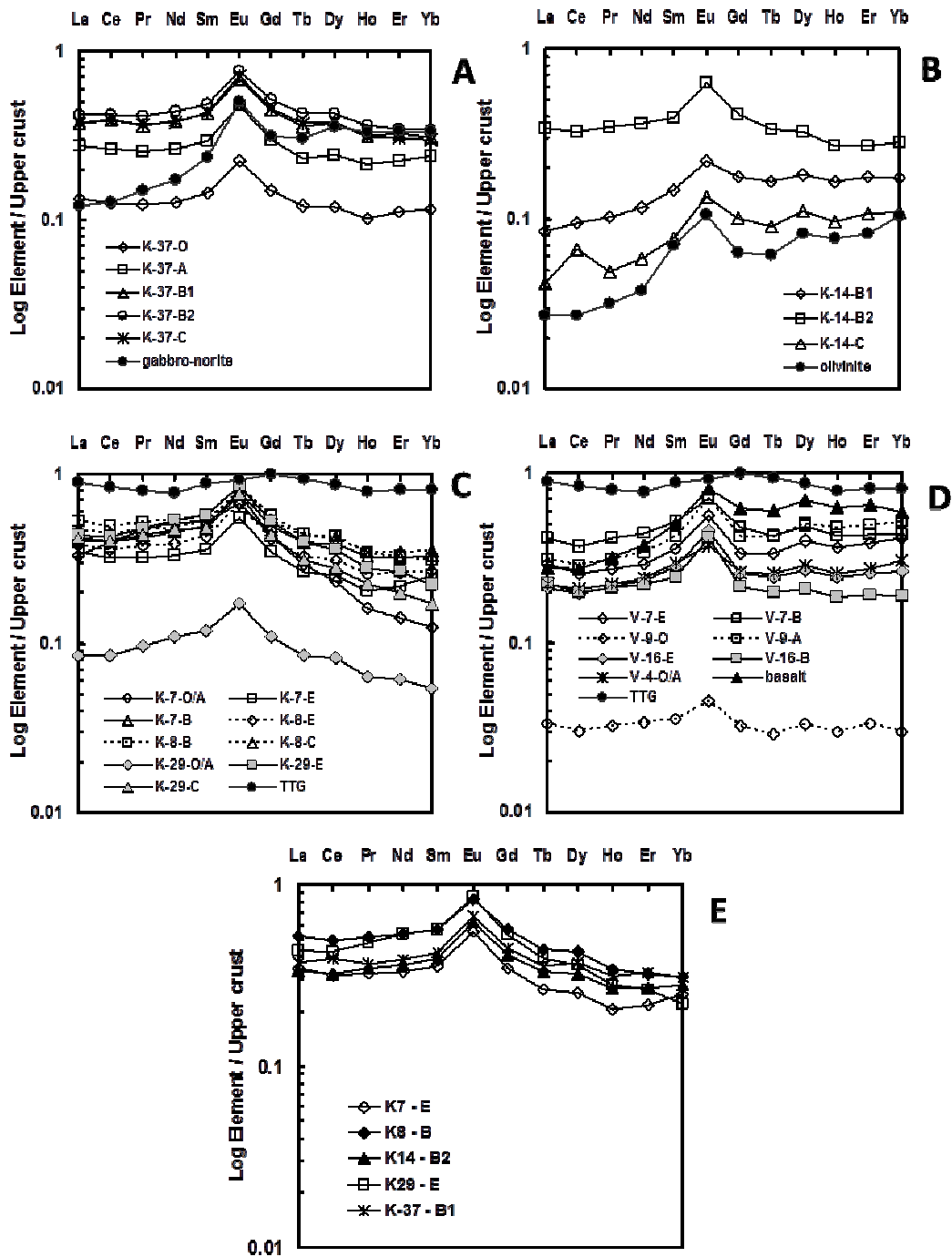


Fig. 6. Upper crust normalized REE patterns for soils from Kivakka intrusion (a, b, c), Vetreny Belt (d), and a mixed diagram on which E and B horizons of different soils are plotted (e). Average composition of the continental crust is taken from Taylor and MacLennan (1985); REE data on rocks of the Kivakka intrusion are from N. Krivolutskaya (unpublished data).

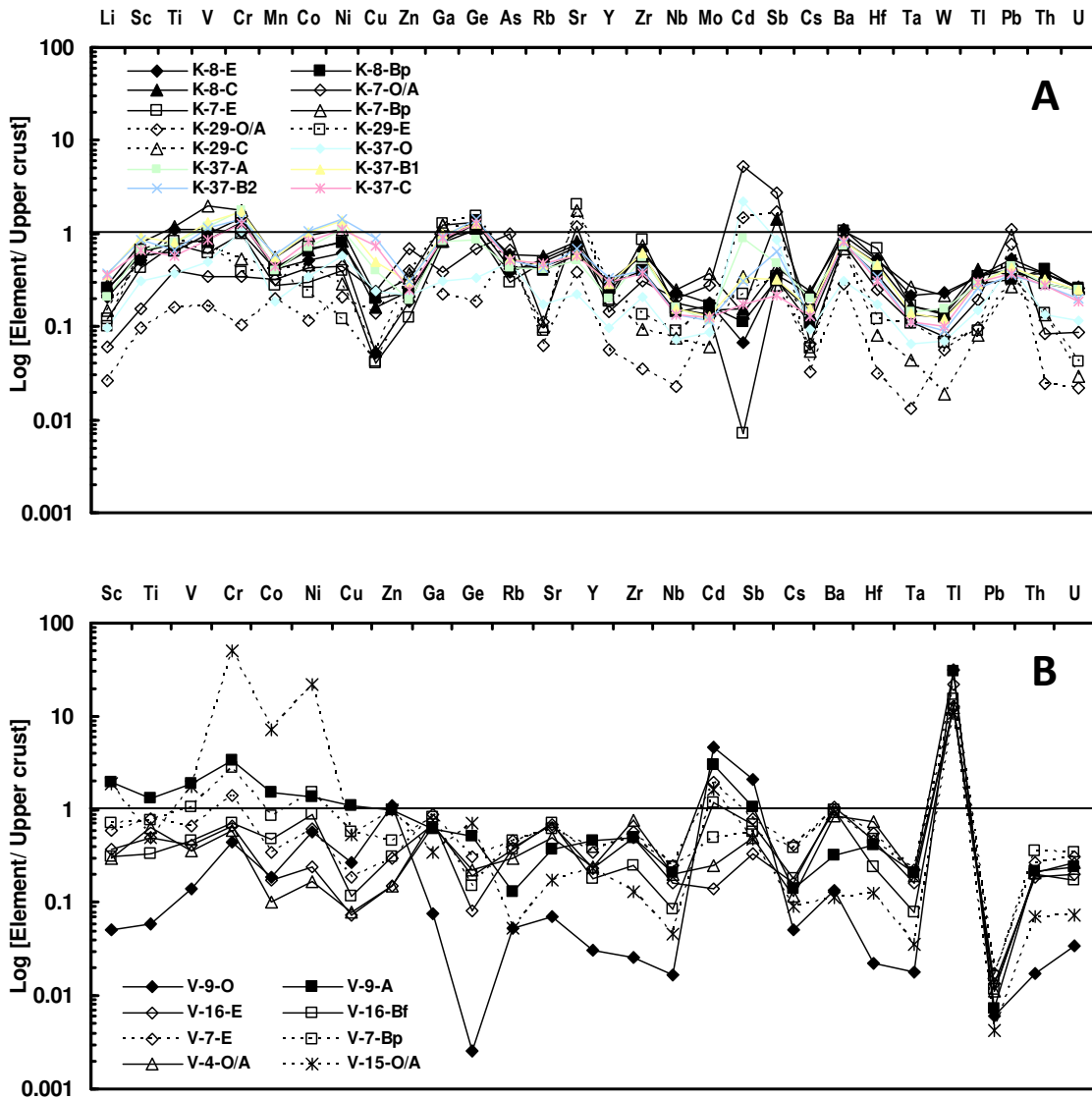


Fig. 7. Upper crust (Taylor and MacLennan, 1985) normalized extended elements patterns for soils developed on both felsic and mafic rocks from the Kivakka intrusion zone (A) and Vetryny Belt zone (B).

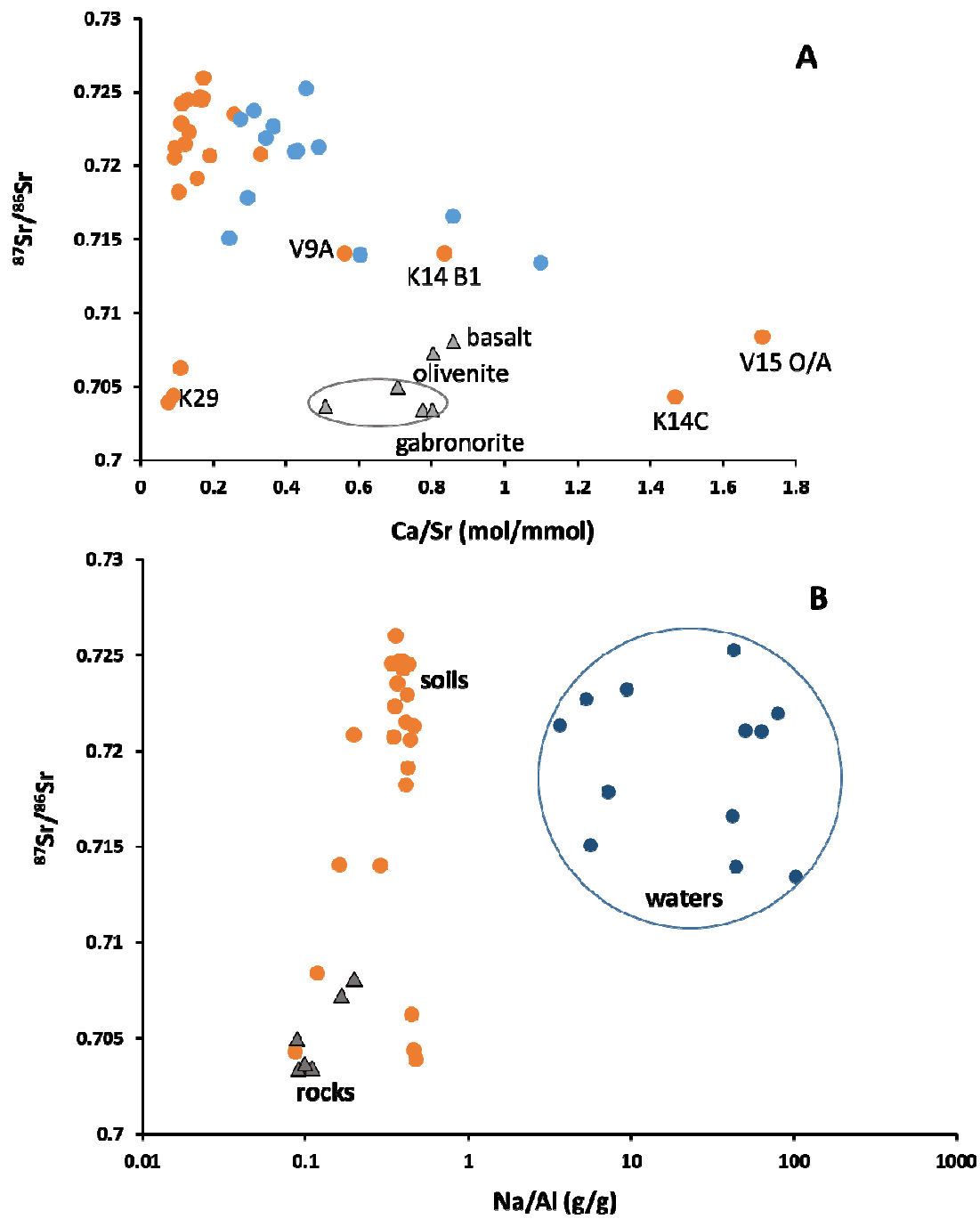


Fig. 8. Sr isotope ratio versus Ca/Sr ratio of soils and rocks (A) and Sr isotope ratio in soils, rocks and waters versus Na/Al ratio as indicator of weathering degree.

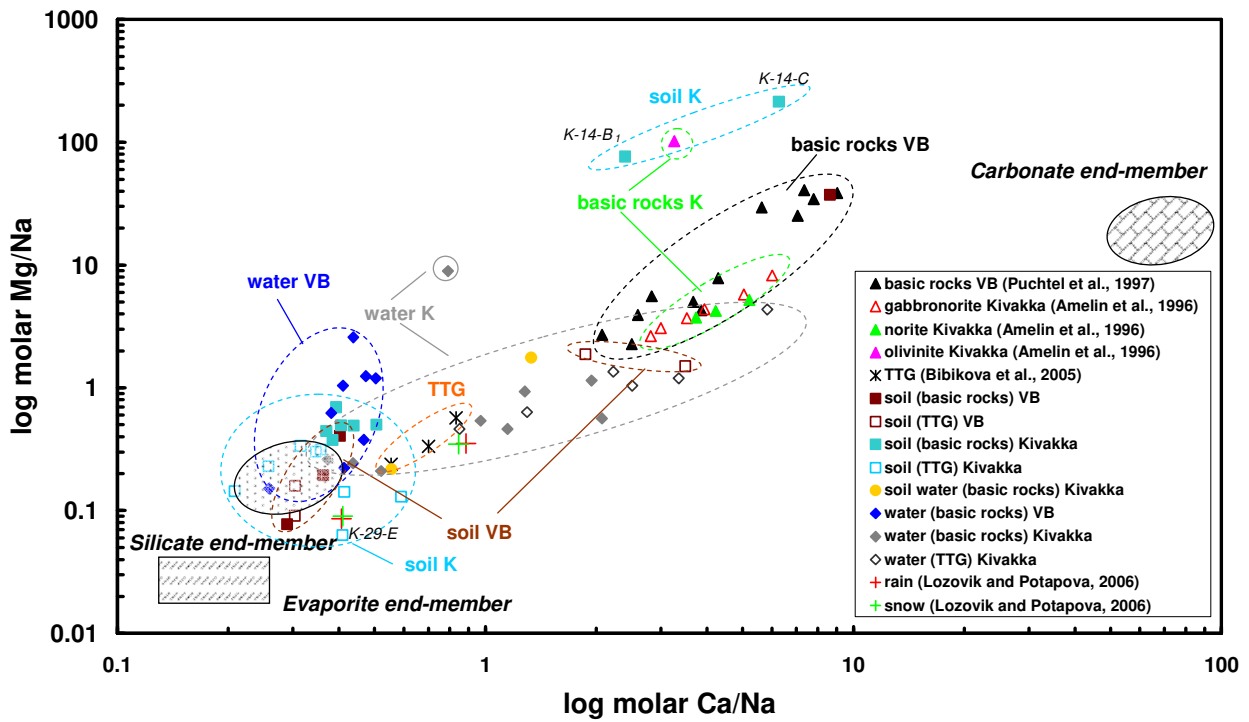


Fig. 9. Ca/Na molar ratios vs. Mg/Na molar ratios showing different materials (soils, rocks and waters) from Kivakka intrusion and Vetreny Belt (VB) zones. The carbonate, silicate, and evaporate end-members are taken from Gaillardet et al. (1999). Atmospheric signatures are calculated from the data reported by Lozovik and Potapova (2006). “VB” and “K” on the diagram stand for Vetreny Belt and Kivakka intrusion zones, respectively. Note that the scale of X and Y axes is different.

Chemical weathering of mafic rocks under granitic moraine in the subarctic

